This is to certify that the
thesis entitled

GENETIC ANALYSIS OF BURIALS FROM THE BUTRINT, ALBANIA TRICONCH PALACE AND MERCHANT'S HOUSE

presented by

CHRISTINA MARIE RAUZI

has been accepted towards fulfillment
of the requirements for the

Master of Science degree in Forensic Science

Major Professor's Signature

11/26/07

Date

GENETIC ANALYSIS OF BURIALS FROM THE BUTRINT, ALBANIA TRICONCH PALACE AND MERCHANT'S HOUSE

By

Christina Marie Rauzi

A THESIS

Submitted to
Michigan State University
in partial fulfillment of the requirements
for the degree of

MASTER OF SCIENCE

Forensic Science

2007

ABSTRACT

GENETIC ANALYSIS OF BURIALS FROM THE BUTRINT, ALBANIA TRICONCH PALACE AND MERCHANT'S HOUSE

By

Christina Marie Rauzi

Molecular analysis of ancient skeletal remains often introduces new information about cultures that cannot necessarily be obtained through anthropological examinations. DNA analysis can be extremely useful when attempting to form hypotheses about culture and burial patterns relating to an ancient burial site such as the Triconch Palace and Merchant's House at Butrint, Albania. The Triconch Palace displays interesting burial configurations consisting of multiple distinct clusters of burials and a large proportion of children present. The analysis of maternally inherited mitochondrial DNA (mtDNA) was conducted on 28 individuals buried within the Triconch Palace, dating to the 5^{th} – 7^{th} century, and 3 individuals from the Merchant's House dating to the 13^{th} – 15^{th} century. Of the 31 individuals analyzed, mtDNA sequence information was obtained for 29. An undifferentiated haplotype in which no clear differences from the reference sequence were present was found for 17 individuals. Six individuals displayed unique sequences, and the remaining 6 shared an mtDNA sequence with at least one other burial. The spatial distribution of mtDNA sequences within the Triconch Palace and Merchant's House combined with information from previous anthropological assessments was used to infer that multiple burial systems occurred in the Triconch Palace at one time rather than only a familial burial pattern as originally hypothesized.

TABLE OF CONTENTS

LIST OF TABLES

LIST OF FIGURES

Introduction

Physical anthropologists often face difficulties when analyzing skeletal material from ancient burial sites. With adequate remains they are usually able to construct a biological profile of an individual that includes characteristics such as age, stature, disease status, and sex. This information is not enough to determine all cultural aspects of the population whose remains are being analyzed, however characteristics of the society, including burial traditions, can be useful in piecing together the history of an archaeological site and provide greater understanding of the people living during a certain era. DNA found in ancient remains serves as an additional tool for answering questions that may remain following anthropological assessment such as the sex of subadults or the familial relationship between individuals unearthed from a burial site. More specifically, mitochondrial DNA (mtDNA) isolated from ancient skeletal material is used to determine whether or not two individuals are maternally related. This information can be combined with an anthropological assessment to determine the burial traditions that were used at that site, such as family plots in which family members are buried next to one another.

Recently, excavations have occurred at the World Heritage Site Butrint, Albania. Excavations include studies of the Triconch Palace and attached Merchant's House, which had a lengthy history and is one of the more prominent structures at the Butrint site. According to the Butrint Foundation Report (2003) it began as a town house in the 2nd century AD and became an elegant palace in the 3rd and 4th centuries. The palace was expanded in roughly 400 AD. By the 5th and 6th centuries, the palace area was occupied by wooden buildings thought to have been built by squatters. During excavation of the

Triconch Palace, skeletal remains were uncovered in various rooms of the palace as well as in the adjacent Merchant's House. Anthropologists at Michigan State University performed skeletal analysis on bones from individuals excavated within the palace. In collaboration with the Anthropology Department at MSU, molecular analysis of mtDNA was performed to determine any possible burial patterns that occurred within the Triconch Palace and Merchant's House. MtDNA sequence data from the individuals excavated within the palace contributes to the anthropological analysis previously performed and provides another piece in the puzzle to understand the history of this unique site.

Butrint, Albania

Current day Albania is a European country roughly the size of Maryland and is located along the Southeast coast of the Adriatic Sea (Figure 1). It shares borders with Greece, Serbia, Montenegro, and the Former Yugoslav Republic of Macedonia (Zickel and Iwaskiv 1994). Albania has a rich history that spans as far back as the 8th century B.C. (Butrint Foundation Website). It is generally thought that the people of Albania originated from the Illyrians who settled in the western Balkans in about 1000 B.C. (Zickel and Iwaskiw 1994). The Illyrians were eventually overtaken by the Romans and Christianity quickly became widespread in the area. The Illyrian lands underwent a series of barbarian invasions from the 4th to 7th centuries by groups including the Goths, Huns, Avars, Serbs, Croats, and the Bulgars, which eventually led to the fall of the Romans in the area (Zickel and Iwaskiw 1994). In the 8th century, the Byzantines came

into power followed by the Ottomans in the 14th century. The area contains many significant archeological sites that reflect occupation by various peoples. Archaeological examination of Albania began in the 1920's when it was studied by an Italian mission (Hodges et al. 2004). According to Zickel and Iwaskiw (1994) in 1944 Albania fell under communist rule. In 1985 the country was ruled by a Stalinist system that forced it into extreme isolation. Due to the political system as well as civil unrest, foreign archaeologists were unable to enter the country to carry out excavations. In 1992, the Albanian people forced the fall of the communist government and shortly after, extensive archaeological excavations were underway.

Figure 1: Map of Albania

The map below depicts the location of Albania in relation to surrounding countries. Butrint is located in southern Albania across from Corfu (Butrint Foundation website).

One of the important archaeological centers of Albania is Butrint. Located near Greece on a small peninsula along the southwest coast of Albania, Butrint was an important stop along major trade routes. Hodges et al. (2004) describe the long and rich history of Butrint. It was inhabited by the Illyrians beginning in approximately the7th century B.C. and was later populated by various groups of people including the Greeks, Romans, Normans, Byzantines, Venetians, Angevins, and Ottomans, each of which is reflected in the archaeological sites within the area. The placement of Butrint on the Straits of Corfu and its central location made it a trade center and also provided natural defenses. The abundant natural resources in the area, including fish and timber also were a source of revenue and power for the town. Hodges and Bowden (2000) described the people and role of Butrint, stating that archaeological evidence suggests that Butrint and its people flourished until the Roman fall. The role of the town as a center of commerce then underwent great change and there is little record of occupation between the mid 7th and the late 9th centuries. Some archaeological findings indicate that there was limited occupation during this time and that the role of Butrint may have changed (Hodges et al. 2004). Inhabitants returned to Butrint in the medieval time period (Hodges and Bowden 2000). The area was once again abandoned in the late Middle Ages when marshes formed, making it uninhabitable (UNESCO.org)

Butrint contains many archaeologically important sites including a baptistery, an amphitheatre, and an Episcopal palace (Figure 2). Butrint became a World Heritage site in 1992 following threats of political instability and possible coastal development (www.history.com). The Butrint Foundation was created in 1993 to aid in the restoration and preservation of the Butrint archaeological site. Civil disturbances in 1997 led to the

decision to place Butrint on the list of World Heritage Sites in Danger. It remained on this list until 2005 (Butrint Foundation Website).

Figure 2: Archaeological Sites in Butrint

Various significant archaeological sites within Butrint are depicted including the Triconch Palace located along the Vivari Channel (Hodges).

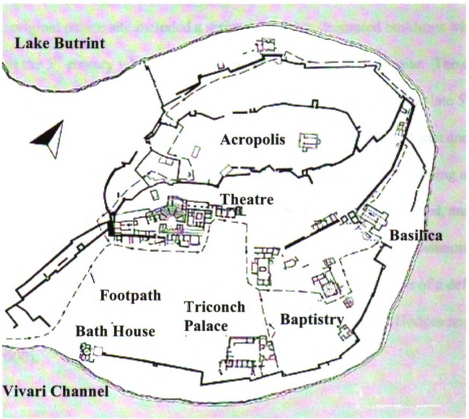

Since extensive excavations of Butrint began in 1994, the site has been well-characterized archaeologically. After excavations, a team of anthropologists from Michigan State University, led by Dr. Todd Fenton, performed an anthropological assessment of burials from the Triconch Palace and Merchant's House (Figure 3).

Hodges and Bowden (2000) present the history of the palace in detail. The Triconch Palace is a complex of buildings located near the Butrint city wall on the northern bank of the Vivari Channel. It was first believed to be a martyrium church, then a paleochristian complex. Currently, it is believed that the Triconch Palace was a domus, a single family palatial dwelling, and eventually became a semi-public building. The palace went through several historical phases that reflect the various roles that Butrint served, as well as the peoples that occupied the city and was built when civilization in Butrint was at its peak. The original palace site included a series of lavishly decorated buildings which existed until the 5th century when a large domus was built on top of the site. The domus included various courtyards and rooms that were elegantly decorated. In the late 5th or early 6th century, construction began to expand the palace to the north and east and to add a Triconch triclinium on the eastern side of the building. The palace remodeling also included plans for a new decoration scheme that was begun but never finished, and a private jetty connecting the property to the Vivari channel, but after the expansion of the palace exterior, the decoration plans were abandoned and the construction of a defensive wall along the channel cut off access from the palace to the waterway (Hodges and Bowden 2000).

Figure 3: Photographs of the Triconch Palace Site

A.) Overhead view of the Triconch Palace B.) View from interior of the Triconch Palace facing the triclinium C.) View of the south side of the Triconch Palace triclinium D.) View of Triconch Palace walls (Hodges).

A.

B.

Figure 3 (continued): Photographs of the Triconch Palace Site

A.) Overhead view of the Triconch Palace B.) View from interior of the Triconch Palace facing the triclinium C.) View of the south side of the Triconch Palace triclinium D.) View of Triconch Palace walls (Hodges).

C.

D.

Following this, the palace began to serve as an industrial building that housed several storage tanks. Hodges et al. (2004) add that several small ovens were discovered along with fish bones and shells, which suggests the building was used to process shellfish and that the storage tanks were used in this industry. The property was then divided by the installation of new walls and may have been sold off in lots (Hodges and Bowden 2000). The tanks described in 2000 were probably used to store shellfish. Near the end of the 6th century the Triconch palace was used as a burial site. This time signifies a change in the burial patterns within Butrint because until the 5th century, dead were buried outside of city boundaries. Burials inside of the property continued until the 7th century, followed by abandonment of the site until the middle of the 9th century. At this point the property was abandoned once again until the Middle Ages when several doors and walls were re-erected. The latest period of use of the site is characterized by post holes and platforms for the construction of at least three timber buildings, as well as a structure with a mortar floor (Hodges and Bowden 2000).

Burials in the Triconch Palace

During excavations of the palace a number of individuals were unearthed within the walls of the palace site and the attached Merchant's House. Figure 4 gives the location of burials within the palace, which were concentrated in rooms along the perimeter of the palace complex. The positions of the burials in relation to each other reveal what are hypothesized to be three or four burial clusters within the palace and another cluster in the southwest corner of the Merchant's House. Archaeological analysis

of time period and anthropological determination of biological profiles revealed that each cluster originated from the same time period and that several of the clusters contained one or two adults and several children. Based on these groupings, it was hypothesized that each cluster could represent a family unit, indicating that some areas within the palace were used as familial burial plots. In addition, some burials share similar directional orientation, which may suggest some type of connection between burials. It is unclear whether or not the interior walls of the palace remained at the time of burial, therefore rooms within the site may have been continuous at the time of burial and familial units may not necessarily be confined to one room.

The first cluster of burials, located in Room N of the palace, consisted of individuals 1188, 1259, 1226, 1224, and 1229, who were children at the time of burial, and 1189 (30 to 45 year-old male), 1185 (adult), and 1225 (35 to 45 year-old male). In addition, burials 1264 (6 to 8 years old) and 1267 (34 week fetus) were located in the same area, but were buried in a north-south orientation rather than the east-west orientation seen in the rest of the burials in the cluster.

The southern portion of the palace contained a concentration of burials situated in two, or possibly three, clusters. Room O held two burial clusters located on opposite sides of the room. Room O East contained four individuals, three of which were analyzed in this study. Individuals 5043 and 1241 were children 1 to 2 years old and 3 to 9 months old, respectively, while burial 1236 was a 23 to 27 year-old female. Five burials (5010; a 35 to 45 year old female, 5189; 12 to 15 years old, 1406; 3.5 to 4 month-old, 5075; 0 to 2 months old, and 5111; 6 months old) were located in Room O West. This cluster was near one with similar orientation in Room T/U but it is unclear based on

spatial information whether the two can be considered one larger grouping. Individuals 1518, 1512, 1509, 1517, and 1502 were located in Room T/U, although only individuals 1518, 1517, and 1502 were analyzed for this research. Individuals 1517 and 1502 were both roughly six months old while 1518 was a male older than 40 years.

Several other burials from the Triconch Palace, in addition to those found within clusters, were analyzed. These were located in rooms by themselves or spatially separated from other burials and were often in a different orientation from other individuals. Individuals not located within clusters included 5641 (late fetal to birth), 5628/5631 (3 to 5 years old), 1456 (neonate), 3126 (6 months old), 3122 (6 months to 1 year old), 1452 (3 to 6 months old), and 1548 (neonate).

The burials located in Room 40 of the Merchant's House, interred in the 13th to 15th centuries, were also part of a cluster. Six burials were located in Room 40, three of which were analyzed here. 3023 and 3060 were teenagers of 12 to 14 and 13 to 15 years old respectively, while 3018 was a 25 to 30 year-old male. These burials were all positioned in a similar north-south orientation.

Figure 4: Map of the Triconch Palace and Merchant's House.

The locations of burials are displayed as well as the rooms within the palace and the attached Merchant's House on the southwest corner. The rooms of the palace are designated by a letter while rooms of the Merchant's House are designated by a number. Burials are indicated with a four-digit number as well as a bold line ending in a dot that depicts the orientation in which the burial was found. The dot indicates the direction of the head. Walls of the palace and Merchant's House are also depicted on the map although it is not know whether or not the walls still stood at the time of each burial.

Figure 4: Map of the Triconch Palace and Merchant's House.

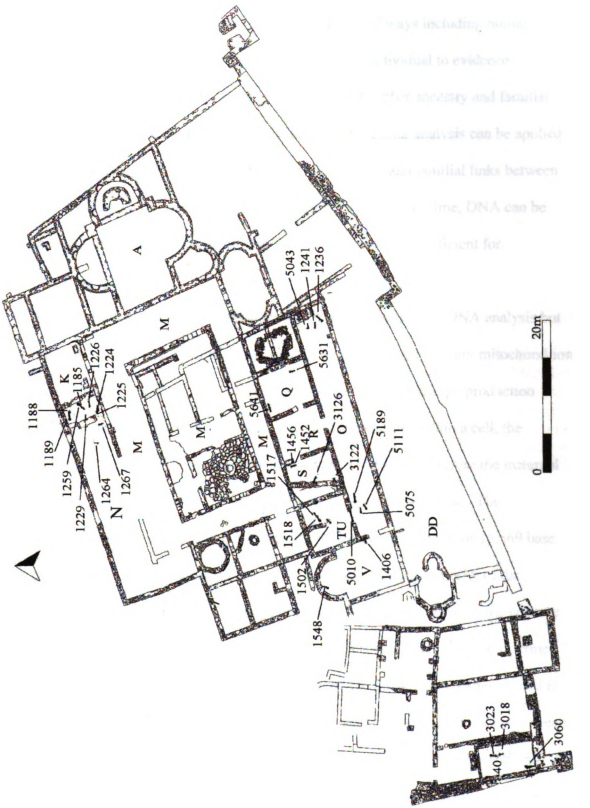

Molecular Analysis of Ancient Remains

Human DNA analysis can be applied in a variety of ways including human identification. In forensic science, DNA data can link an individual to evidence recovered from a crime scene, determine paternity, and decipher ancestry and familial lineages, among many other things. In a similar way, molecular analysis can be applied to ancient remains to learn more about the individual burials and familial links between burials. This application presents a unique challenge because over time, DNA can be degraded and damaged, making it difficult to recover in amounts sufficient for informative analysis.

Nuclear DNA and mitochondrial DNA can both be utilized in DNA analysis but have different applications. MtDNA is present in multiple copies in every mitochondrion in the body. Mitochondria are the cell organelles responsible for energy production through oxidative phosphorylation. Multiple mitochondria exist within a cell, the quantity depending on cell type. MtDNA is maternally inherited therefore the maternal lineage of a family will possess the same mtDNA sequence or haplotype. The mitochondrial genome is configured as a circular molecule and consists of 16,569 base pairs that make up 37 genes (Anderson et al. 1981). Although the majority of the mtDNA contains genes related to energy production, there are also areas of the genome that do not code for a gene product. This non-coding portion of the sequence is termed the control region because it directs replication and transcription of the molecule and is the area most often utilized in molecular analysis because much of the variation between individuals lies there (Horai and Hayasaka 1990). The control region is divided into hypervariable regions I and II (HVI and HVII) in humans. HVI refers to the sequence

from nucleotide position 16024 to position 16365, while HVII refers to sequence between position 73 and position 340 (Greenburg et al. 1983). Anderson et al. described the sequence of the mtDNA genome in 1981, to which subsequent edits were made, resulting in the Cambridge Reference Sequence which has come to serve as a reference tool for analyzing mtDNA sequences, as individual haplotypes are referred to based on their differences from the CRS.

Nuclear DNA and mtDNA each have advantages depending on the type of material being analyzed. Nuclear DNA analysis is used in situations where a high quality DNA source is accessible and a relatively large amount of DNA is present. It can yield individualizing information and be used to link a person to both maternally and paternally related relatives. The use of nuclear DNA becomes nearly impossible if extensive degradation has taken place and/or DNA exists in a very low copy number. MtDNA analysis is used when nuclear DNA cannot be obtained from a sample, which is often the case in analysis of archaeological specimens such as those examined in this research. MtDNA analysis is the preferred method for ancient skeletal remains for various reasons. Foran (2006) examined a number of factors that influence the degradation of nuclear versus mtDNA. Since multiple mitochondria are present in every cell and each contains multiple copies of mtDNA, the number of mtDNA copies is much larger that of single copy nuclear DNA. Different stretches of nuclear DNA may or may not be resilient to degradation depending on the location within the nucleus and the transcriptional activity of each sequence region. Nuclear DNA may also be vulnerable to exonuclease attacks because of its linear form. In contrast, the circular form of mtDNA may provide protection from exonucleases since there are no free ends for the enzymes to attack. In

addition, mitochondria are theorized to be the result of a prokaryote being engulfed by a eukaryotic cell. If this is the case, the cell membrane of the prokaryote must have been resistant to digestion by the cell to remain and take on the function of a mitochondrion, and probably provides the DNA inside the organelle more protection than DNA within the nucleus.

Challenges of Ancient DNA Analysis

The success of molecular analysis of ancient remains is highly dependent on the amount of DNA left in the sample and the degree to which any remaining DNA has been damaged. The degree of deterioration of DNA is influenced not only by the age of the sample, as an increase in time may allow degraded positions to accumulate, but also the environmental conditions to which the remains are exposed such as temperature, pH, humidity, and number and type of microorganisms present. According to Lindahl (1993), DNA present in ancient skeletal remains binds to hydroxyapatite within the bone structure, which helps to slow the rate of degradation. Any environmental factors that interfere with the hydroxyapatite content of the remains can render the DNA more prone to damage. Low pH and microorganisms can degrade the structural integrity of the bone (Collins et al. 2002), which may indirectly affect the DNA within.

The limited quantity of endogenous DNA that may be present in an ancient sample is the main concern when analyzing skeletal remains. If the quantity of DNA is not sufficient, analysis may not be possible. This challenge can be overcome by use of the polymerase chain reaction (PCR). PCR makes use of a thermostable DNA

polymerase, a set of two oligonucleotide primers that are complementary to a portion of the template DNA, and a series of thermal cycles. The PCR process results in an exponential amplification of a region of the template DNA that sits between the two primers, and ideally, creates a sufficient quantity of DNA so that further analysis may be conducted. If very low copy number DNA is used as template, a large number of thermal cycles may be needed for sufficient amplification. The sensitivity of PCR can be increased and the occurrence of nonspecific binding can be decreased through the use of a nested PCR technique. Nested PCR involves using approximately 20 to 35 cycles with a specific primer set. Depending on the amount of product visualized after the first round of PCR, a second PCR is performed for 15 to 20 cycles. The second PCR utilizes a set of primers that is internal to the set used in the first round of PCR. Semi-nested PCR is one variation of nested PCR in which only one of the second primers is internal to the first set, while the other primer remains the same. Both nested and semi-nested techniques increase amplification rates when DNA exists in a low quantity.

Postmortem DNA damage and degradation can occur in a variety of manners. Living organisms contain mechanisms that prevent and repair DNA damage, but no such mechanism exists once an organism has died (Lindahl 1993). Hydrolysis of DNA results in a breakdown of the N glycosyl bond between the ribose sugar and the base when water is present. Oxidative damage by hydroxyl or superoxide radicals can modify bases or cause distortion of the DNA helix. This is a concern in mtDNA analysis because oxidation occurs more readily in the mitochondria after death (O'Rourke et al. 2000). Strand breaks, baseless sites, miscoding lesions and crosslinked bases are other forms of damage that may exist along a DNA strand and can be caused by oxidation or other

chemical degradation processes. In addition, individual bases within a sequence may be altered by depurination, depyrimidination, and deamination (O'Rourke et al. 2000). In most cases of DNA damage, the altered strand is unable to be amplified because the polymerase cannot recognize the base or cannot replicate across a damaged area. This results in a low amount of amplification product. In cases of deamination, the damaged base is recognized by the polymerase, but replication results in the wrong base being inserted into the amplification products (O'Rourke et al. 2000). Deamination occurs spontaneously in cytosine (C) residues and results in a uracil (U) residue. The polymerase reads the U as thymine (T) in a DNA strand and the result is a C to T transition or a G to A transition if the opposite strand is read. Adenine can also be deaminated to hypoxanthine, which the polymerase reads as guanine, resulting in an A to G transition (Gilbert et al. 2003). Miscoding lesions appear to be more frequent at certain nucleotide positions along the mitochondrial genome (Gilbert et al. 2003). These positions as well as any area where a miscoding lesion is present may be problematic in mtDNA analysis because interpretation of an mtDNA haplotype requires the examination of sequence differences between two individuals. Miscoding lesions lead to a change in the base that is present at one position or result in ambiguous sequence, increasing the difficulty of interpretation. Sequence ambiguities can also be a result of heteroplasmy, in which a living individual has two bases present at a certain nucleotide position within their mtDNA haplotype. Heteroplasmy is fairly uncommon and can often be tissue specific (Theves et al. 2006).

Another problem that is encountered in ancient DNA analysis is PCR inhibition. According to Wilson (1997), PCR inhibition occurs in four forms. Inhibitors may

interfere with cell lysis during DNA extraction, degrade nucleic acids, and may affect polymerase activity. The last of these is a great concern when analyzing ancient skeletal remains. Inhibitors are thought to interfere with the polymerase during PCR by directly binding and rendering it inactive, or by binding to DNA, preventing polymerase binding and replication, and are present in a wide variety of substances including body fluids, food constituents, and environmental compounds such as soil (Wilson 1997).

Contamination by higher quantity DNA can also be problematic when manipulating old and degraded samples. The quantity and quality of DNA present in ancient samples is often very low compared to DNA from researchers in the lab. If correct precautions are not taken, modern DNA contamination can be preferentially amplified in PCR. The risk of contamination is reduced by making use of two different, dedicated rooms for pre-amplification and post-amplification procedures. Contamination may also be prevented by UV irradiating all reagents and tubes, wiping down work areas with 10% bleach solution, and performing extractions in a sterile hood. Personal protective equipment in the form of surgical masks, disposable sleeves, lab coats, and two pairs of latex gloves should also be worn. Any exogenous DNA that exists from handling of skeletal samples during excavation or anthropological examination should be removed through bone washing protocols as well as by removal of the outer surface of the sample prior to drilling for powder (Edson et al. 2004). The authenticity of sequences obtained can be determined by processing at least two bones from each individual on separate occasions and using the sequences to generate a consensus sequence. The haplotype of the DNA analyst that processed the samples should also be known and compared to sequences obtained from the skeletal remains or any contaminating sequences found to

rule out contamination during handling. Finally, the use of extraction blanks and proper negative controls throughout analysis ensure that contamination is not present in reagents or materials.

Project Goals

The goal of the research presented here was to conduct molecular analysis of the skeletal remains excavated from the Triconch Palace and Merchant's House in Butrint, Albania so as to generate mitochondrial DNA sequence data for each individual. Analysis of similarities and differences between haplotypes provide information about the maternal relatedness of individuals in various rooms of the palace. The combination of molecular data and previous anthropological analysis were utilized to determine possible burial patterns that occurred within the palace during the 5th to 7th centuries and the 13th century as well as to make inferences about the social culture in Butrint during these time frames.

Materials and Methods

A total of 31 burials from the excavation of the Triconch Palace in Butrint, Albania were analyzed in this research. Individuals examined included those excavated from Rooms N, O, Q, S, T/U, and V of the palace (Figure 4) as well as three burials from Room 40 of the adjacent Merchant's House. Prior to this research, archaeologists estimated that the skeletal samples from the palace date to between the fifth and seventh centuries A.D., while the burials excavated from the Merchant's House date to between the thirteenth and fifteenth centuries A.D. The bones from each burial were also assessed by anthropologists to create a biological profile consisting of age and sex estimate. Seven of the burials were adults while the rest were subadults, 14 of which were infants. For 26 of the burials, multiple bones from an individual were used for analysis. Complete biological profiles and bones types are detailed in Table 1. These included fibula, radius, humerus, tibia, ulna, femur, rib, frontal fragment of the skull, and petrous portion of the skull. Long bone samples taken from infants included the entire length of the bone, while those from older children and adults consisted of a cross section taken from the shaft measuring approximately two to six inches long. In cases where more than one bone from an individual was analyzed for mtDNA, samples consisted of at least one long bone as well as a petrous portion of the skull, if available.

Table 1: Bones Processed for DNA

Bones for which mtDNA analysis was attempted as well as the location of sample within the palace and biological profile of individual. Rooms correspond to Figure 4. Burial numbers were designated by archaeologists and correspond to those in Figure 4 as well.

Room	Burial	Bone Type	Sex	Age
N	1185	fibula shaft		adult
N	1187/1189	right radius midshaft	male	30 – 45 yrs
		right fibula midshaft		
N	1188	left humerus shaft		11 – 13 yrs
		right petrous portion		
N	1224	left petrous portion		3 – 4 yrs
		right humerus midshaft		
N	1225	right petrous portion		3 – 4 yrs
		left tibia midshaft		
N	1226	right fibula	male	35 – 45 yrs
		left ulna midshaft		.
N	1229	left petrous portion		3 – 6 mos
		humeral shaft		
N	1259	left femur midshaft		10 – 12 yrs
N	1264	tibia cortical fragment fr. Distal end		6 – 8 yrs
		fibula midshaft		
O	1236	fibula midshaft	female	23 – 27 yrs
		left ulna midshaft		
O	1241	right petrous portion		3 – 9 mos
		fibula midshaft		
O	1267	petrous portion		fetus 34 wks
		tibia fragment		
O	5043	right petrous portion		1 – 2 yrs
		fibula midshaft		
O	5075	left petrous portion		0 – 2 mos
		right rib		
O	5111	left petrous portion		6 mos
		femur midshaft		
O	5189	fibula midshaft		12 – 15 yrs
Q	5628/5631	r. petrous portion		3 – 5 yrs
		r. femur fragments		
Q	5641	right petrous portion		Late fetal – birth
S	1452	l. femur fragment		3 – 6 mos
S	1456	r. petrous portion		neonate
		r. clavicle		
S	3122	r. tibia		6 mos – 1 yr
		frontal fragment		
S	3126	l. petrous portion		6 mos
		fibula fragment		
T/U	1502	left ulna		6 mos – 1 yr

Table 1 (continued)

Room	Burial	Bone Type	Sex	Age
		tibia		
T/U	1517	right petrous portion		6 mos
		right ulna		
T/U	1518	humeral cortical frag	male	40+ yrs
		humeral cortical frag		
		fibula midshaft		
T/U	5010	fibula midshaft	female	35 – 45 yrs
		humerus midshaft		
V	1406	l. petrous portion		3.5 – 4.5 yrs
		l. femur		
V	1548	r. petrous portion		neonate
		l. tibia		
MH	3018	petrous portion		12 – 14 yrs
		rib		
MH	3023	petrous portion	male	25 – 35 yrs
		femur		
MH	3060	unknown*		13 – 15 yrs
		unknown*		

*Bone types were not anthropologically determined.

Figure 5: Photographs of Select Burials

Eight skeletons that were among the individuals analyzed in this research are displayed in the following photographs (A – D). Location of each burial within the Triconch Palace as well as the biological profile is included.

A. Burial 1518
Located in Room T/U
Male, 40+ years old

Figure 5 (continued)

B. Burial 5010
Located in Room T/U
Female, 35 – 45 years old

Figure 5 (continued)

C. Burials 1188 and 1189
1188: Located in Room N
11 – 13 years old

1189: Located in Room N
Male, 30 – 45 years old

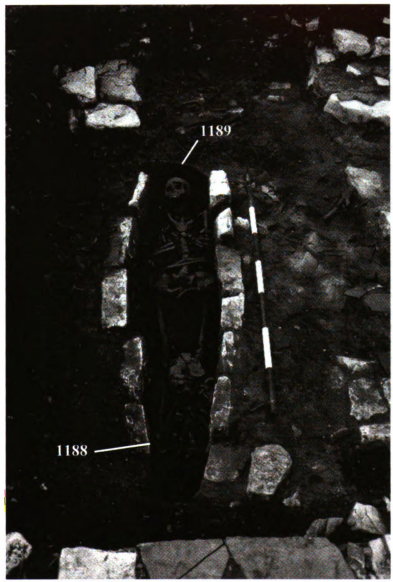

Figure 5 (continued)

D. Burials 1224, 1225, and 1226 (from left to right)
1224: Located in Room N
3 – 4 years old

1225: Located in Room N
3 – 4 years old

1226: Located in Room N
Male, 35 – 45 years old

Bone Preparation

Early in this research, bone samples were prepared for drilling by removing as much surface dirt as possible using filter sterilized water and sterile cotton swabs. The surface of the bone was swabbed with filter sterilized bone wash (20mM Tris pH 8, 10mM EDTA, 0.5% SDS) on a sterile cotton swab. The sample was then allowed to air dry. This cleaning process worked sufficiently well for bones that did not contain much soil on the surface or in any cavities, but was problematic for samples with a large amount of soil present. Vibrations caused by drilling dislodged remaining soil, which fell into bone powder that was being collected. To remedy this, an extra cleaning step was added prior to swabbing with water and bone wash. A 10 % bleach solution and Liquinox detergent were applied to a small glassware brush, and the brush was rinsed with sterile water so only a small amount of detergent remained on the brush. Wetted samples were scrubbed with the brush, then rinsed with sterile water until all surface soil and all or most of the soil present in the cavities was removed. This was followed by a thorough rinsing with filter sterilized water. The samples were placed in weigh boats and allowed to air dry overnight in a drawer.

Prior to sampling, bone wash, Milli-Q water, and digestion buffer (20mM Tris pH 8, 50 mM EDTA, 0.5% SDS) were filter sterilized. One-sixteenth inch titanium drill bits, 3/8 inch aluminum oxide grinding stones, a sanding wheel, and drill parts were soaked in a solution of 10% bleach, Liquinox detergent, and water for at least ten minutes. The drill accessories were then scrubbed with more 10% bleach and detergent with a glassware brush. This was followed by a thorough rinse with Milli-Q water and 70%

ethanol. Once dry, the drilling materials along with a Dremel tool, weigh boats, weigh paper, sterile 1.5 mL microcentrifuge tubes, sterile cotton swabs, and hemostats were UV irradiated for 10 minutes. All materials were transferred to a UV sterilized Cleanspot PCR Workstation and exposed to constant UV irradiation while not in use. Bones were drilled in a hood that had been UV irradiated for 15 minutes immediately prior to use. Using the Dremel tool set to a low or medium speed and fitted with a 1/16 inch titanium drill bit, a small indentation, roughly one millimeter deep, was drilled into the bone surface. Up to three additional indentations adjacent to the first were drilled in this manner, to create an area large enough to collect powder. The area surrounding the indentations was swabbed with a sterile cotton swab soaked in bone wash, followed by a dry cotton swab, to remove any contaminating bone powder generated by the first drilling step. This double swabbing procedure was repeated three times and the area was allowed to air dry. The Dremel tool was wiped down with 70% ethanol to remove any bone powder and was fitted with a sterile 1/16 inch titanium drill bit. The indentations made previously were drilled at a medium to high speed to generate bone powder from the cortical bone. Twenty to fifty milligrams of powder was collected on a piece of weigh paper, transferred to a sterile 1.5 mL microcentrifuge tube, and weighed.

This procedure was performed on thicker long bones from older children and adults, as well as all petrous portions, however some bones were too small or did not contain a layer of cortical bone deep enough to drill into and generate powder, so an alternative protocol was implemented, primarily for use on long bones from infants. The outer surface of the area to be sampled was sanded lightly at a low to medium speed using the Dremel tool fitted with a sterile sanding wheel. The area was swabbed with

bone wash and a dry swab using the technique detailed above to remove surface powder. The Dremel tool was fitted with a sterile 3/8 inch aluminum oxide grinding stone. Bone powder was generated from cortical bone by grinding the surface with the Dremel tool set at a medium speed, and the powder collected and weighed in the manner described above. Following both sampling procedures, a reagent blank was prepared by adding 200 µL of sterile digestion buffer and two µL of proteinase K (20 mg/mL) to a sterile 1.5 mL microcentrifuge tube. Four hundred to 500 µL of sterile digestion buffer and 4 to 5 µL of proteinase K were added to each tube of bone powder collected, which was vortexed vigorously for at least 30 seconds. Bone powders and associated reagent blanks were incubated overnight at 55°C.

DNA Extraction

DNA extractions were performed in a laminar flow hood by adding an equal volume of saturated phenol and vortexing for thirty seconds. Samples and reagent blanks were vortexed thoroughly, and centrifuged at 14,000 rpm for five minutes. The aqueous layer was transferred to a sterile 1.5 mL microcentrifuge tube. If the aqueous extract was discolored (usually brown, yellow, or pink) a second phenol extraction was undertaken. The process was then repeated with an equal volume of chloroform. The aqueous layer was transferred to a UV irradiated Microcon YM-30 filter column (Millipore) and 100 µL of filter-sterilized Tris EDTA (TE—10 mM Tris pH 8.0, 1 mM EDTA) was added. The sample was centrifuged at 13,000 X g for ten minutes. The filtrate was discarded, 300 µL of sterile TE was added to the column, and the sample was centrifuged at 13,000

X g for ten minutes. The TE wash was repeated and the retenate was brought to 20 µL by adding an appropriate volume of TE to the membrane. After sitting undisturbed for five minutes, the column was inverted into a new Microcon collection tube and centrifuged for three minutes at 1,000 X g to collect the retenate. DNA samples and reagent blanks were stored at -20 °C.

DNA Amplification

HVI was amplified using primers F15989 and R16207 while HVII was amplified using F15 and R285 in the first round of PCR. A semi-nested PCR technique was used when necessary by replacing F15989 and F15 with F16057 and F82, respectively. Primer sequences can be found in Table 2. PCR tubes, sterile water, and HotMaster buffer (Eppendorf) were UV irradiated for ten minutes. Bovine serum albumin (BSA) at100 µg/µL was UV irradiated for five minutes. Sets of PCR reactions included a negative control with no DNA template added, a positive control, as well as the reagent blank that corresponded to each set of samples. PCR reactions consisted of 2 µL of HotMaster buffer, 0.2 mM each of deoxynucleoside 5'-triphosphates, 0.4 µL each of a forward and reverse primer (20 µM), 0.6-0.8 µL of 100 µg/µL BSA, and 1U HotMaster Taq polymerase (Eppendorf). The reactions were brought to 20 µL with filter sterilized water. One µL of DNA template from each sample was added to the corresponding reaction tube. One to 20 dilutions were also prepared. One µL of reagent blank and positive control template were added to the corresponding reactions. The cycling parameters for the non-nested round of PCR included a denaturation step at 94°C for 2

minutes, followed by 35 cycles of denaturation at 94°C for 30 seconds, primer annealing at 56 °C for 1 minute, and extension at 72 °C for 1 minute. Five μL of all PCR products were electrophoresed on a 2% agarose gel, stained with ethidium bromide, and visualized with UV light to determine the amount of product present. If little or no product was visible on the gel, semi-nested PCR was performed.

Table 2: HVI and HVII Primer Pairs

Primers used for standard and semi-nested PCR amplifications. Primer names and sequences are shown. F indicates a forward primer while R indicates a reverse primer.

HVI		HVII	
Non-nested Primer Pair		**Non-nested Primer Pair**	
F15989 5'-cccaaagctaagattctaat	R16207 5'-acttgcttgtaagcatgggg	F15 5'-caccctattaaccactcacg	R285 5'-gttatgatgtctgtgtggaa
Semi-nested Primer Pair		**Semi-nested Primer Pair**	
F16057 5'-aagtattgactcacccatca	R16207 5'-acttgcttgtaagcatgggg	F82 5'-atagcattgcgagacgctgg	R285 5'-gttatgatgtctgtgtggaa

Semi-nested PCR reactions were prepared using a primer set internal to the first for both HVI and HVII. One μL of the non-nested PCR product was added to a reaction as template. The reagents and cycling parameters remained the same while the number of cycles was reduced to 15 to 20 depending on the amount of DNA visualized on the agarose gel following preliminary PCR. If bands were present, but determined to be insufficient for sequencing, 15 to 17 cycles were used. If no bands were visualized, 20 cycles were utilized. Five μL of the nested PCR products were electrophoresed on a 2% agarose gel, stained, and visualized. In cases where sufficient DNA was present, the samples were prepared for sequencing. If bands were seen in a negative control and/or

reagent blank a new PCR reaction was prepared using only 15 to 17 cycles. Negative controls and reagent blanks in which a band was visualized were also sequenced to determine the source of contamination.

DNA Sequencing

The remaining PCR reaction was transferred to a Montage PCR Centrifugal Filter device (Millipore) for purification. Three hundred μL of TE were added to the top of the column, which was centrifuged for 15 minutes at 1,000 X g. The retenate was brought to 10 – 20 μL by adding the appropriate amount of TE to adjust to the optimal amount of DNA template needed for sequencing as suggested by the CEQ Dye Terminator Cycle Sequencing Chemistry Protocol. Sequencing reaction consisted of 4 μL of CEQ DTCS Quick Start Master Mix, 1 μL of a 20 μM forward or reverse primer used in the semi-nested or unnested PCR, approximately 6.5 ng (50 fM)of DNA template, and filter sterilized water to bring the final volume to 10 μL.

Sequencing parameters consisted of 30 cycles of denaturation at 94°C for 20 seconds, primer annealing at 50 °C for 20 seconds, and extension at 60 °C for 4 minutes. In previous research (Murray 2006), it was determined that reverse primer 16207 required denaturation at 96 °C, annealing at 61.5 °C, and extension at 65 °C, hence these parameters were used in the current research. A stop solution was prepared using 10 μL 3M NaOAc, 1 μL 100mM EDTA pH 8.0, and 5 μL 20mg/mL glycogen (per 10 reactions). Two and one-half μL were added to each sample, followed by 30 μL cold 95% ethanol. DNAs were vortexed and centrifuged at 14,000 rpm for 15 minutes. The

supernatant was pipetted off and the pellet was washed twice by adding 100 μL of cold 70% ethanol, centrifuging for 5 minutes at 14,000 rpm, and removing the supernatant. Pellets were vacuum dried for a minimum of 20 minutes, resuspended in 40 μL of Sample Loading Solution (Beckman), and vortexed for at least 20 seconds.

DNAs were loaded onto a 96 well CEQ sample plate (Beckman), overlaid with a drop of mineral oil, and separated on a CEQ 8000 Genetic Analyzer (Beckman) using the LFR-1-60 program (50 °C capillary temperature, denature at 90 °C for 120 seconds, inject at 2.0kV for 15 seconds, and separate at 4.2kV for 60 minutes). Sequences were analyzed using the CEQ analysis software and were uploaded into BioEdit (Hall 1999). Sequence was aligned with a reference sequence (Anderson et al. 1981) and polymorphisms were noted and recorded.

Results

Bone Sampling

A total of 58 bone samples were collected for mtDNA analysis from the Triconch Palace and Merchant's House, while bone powder was obtained and processed from 51 samples. Of the 58 samples available, the type of bone used for analysis most often was petrous portion (29% of the time), followed by fibula (14%), humerus (10%), femur (10%), tibia (9%), ulna (7%), rib (3%), radius (2%), and frontal portion of the skull (2%). Bones of unknown skeletal origin were used 3% of the time. One clavicle was available but did not contain sufficient bone mass to be drilled for use in further analysis.

Petrous portion and large long bones were the skeletal samples of preference because they contain a greater proportion of cortical bone that is thought to offer more protection for DNA that may be present. The larger long bones were generally the most simple to prepare for DNA analysis because they were easy to clean and powder could be collected from a cross-section of the shaft. Most of the skeletal remains were from subadults and the small size and small amount of cortical material present in the shaft of the long bones made many difficult or impossible to drill. The seven skeletal samples that were unable to be analyzed were from infants or very young children did not contain adequate bone mass for processing. Petrous portions proved to be more problematic to clean than long bones because they contained crevices that trapped dirt and made it difficult to remove, however, petrous portions from small children were easier to drill

than long bones as they were thicker, providing sufficient area for drilling and collecting powder.

DNA Extraction

During drilling and collection of bone powder for downstream DNA analysis, great care was taken to sufficiently clean the material so that only bone powder was collected, however occasionally, dirt became mixed with the powder in samples that contained a large amount of debris. As a result, the addition of digestion buffer and proteinase K produced a colored bone powder suspension that was darker than what was seen if only bone powder was present. The majority of these samples produced colored extracts ranging from yellow, to red, to dark brown after the phenol extraction was performed. When colored extracts were encountered, 2 reextractions with phenol were done, although much of the time the extra phenol steps did not remove the majority of the coloration. Pushing the extracts through a Microcon filter centrifugation device and washing 2 times with TE removed the pigmentation in the light to medium colored samples, but in dark brown samples, a brown residue remained on the filter and was eluted off the filter along with the final DNA sample. The brown residue did not seem to affect downstream amplification of the DNAs.

In some samples, white debris accumulated on the Microcon filter after centrifugation. As the DNA was eluted off the filter it adhered to the filter and was not visible in the final DNA sample. The debris was observed from petrous portions of individuals 1225, 1241, 5111, and 1456, ulna of individual 1517, humerus of individual

1518, humerus of individual 5010, and femur of individual 1406. The white substance did not seem to be inhibitory because for at least one of the hypervariable regions PCR product was obtained from each bone. Only DNA from the petrous portion of burial 1241 failed to amplify in all attempted PCRs. In some cases Microcon YM-100 filter columns were utilized according to the manufacturer's protocol rather than YM-30s. It was found that this resulted in higher amplification success in discolored samples presumably because PCR inhibitors were allowed to pass through the membrane. No white or brown residue remained on the filter when YM-100 columns were used.

Mitochondrial DNA Amplification

An initial PCR was conducted for each skeletal sample for both HVI and HVII using a neat reaction with 1 μL of DNA per 20 μL as well as a 1:20 dilution. There was roughly equal amplification success of HVI compared to HVII in the first (unnested) round of PCR; twelve percent of the 51 bone samples produced a HVI product compared to 14 % for HVII. Larger numbers of PCR cycles often resulted in product in a negative control. This was remedied by lowering the cycle number to between 15 and 18 in semi-nested PCR.

The amplification success rate increased when a semi-nested PCR was performed, resulting in a 73% rate overall for HVI and a 76% amplification rate for HVII. An example of a semi-nested PCR product is given in Figure 6. In cases where the first attempt at amplification was unsuccessful after using the semi-nested technique, subsequent amplification attempts were performed, further increasing the number of

samples that gave a PCR product. The final amplification percentages for HVI and HVII were 88% and 82%, respectively.

Figure 6: Semi-nested PCR

(a) Two percent agarose gel showing product from the first round of PCR. No bands are visible except the positive control in lane 15. (b) Two percent agarose gel showing product from a semi-nested PCR. Lane 1 contains a 100 base pair ladder. The negative control and reagent blank are in lanes 2 and 3. Lanes 4 through 14 in both (a) and (b) contain DNA amplified from the same bones.

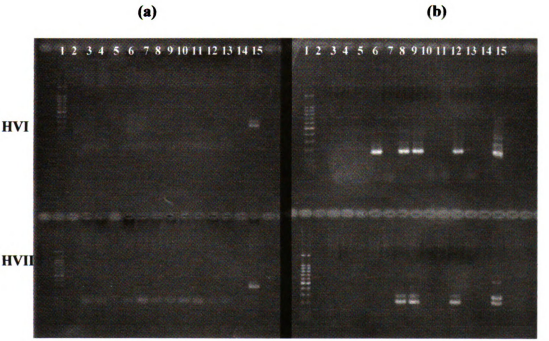

Different types of bone showed different rates in amplification success in amplification. Bones for which DNA from HVI amplified in the first round of PCR include radius, fibula, ulna tibia, and humerus. DNA from petrous portion, fibula, radius, humerus, and ulna amplified in the first round of HVII PCR. Bones that did not amplify in the non-nested PCR were femur, rib, and frontal portion of the skull. Overall, the bone

types that amplified at the greatest frequency for HVI were radius (1 of 1 sample) femur (6 of 6), rib (1 of 1), ulna (4 of 4) and frontal portion of the skull (1 of 1), followed by fibula (6 of 8), humerus (5 of 6), skull petrous portion (14 of 17), and tibia (4 of 5). The overall HVII amplification efficiencies were: radius (1 of 1), rib (1 of 1), frontal portion of the skull (1 of 1), humerus (5 of 5), fibula (7 of 8), petrous portion (13 of 17), tibia (4 of 5), ulna (3 of 4), and femur (4 of 6). Table 3 details drilling and amplification success according to bone type and age of individual.

Despite repeated amplification attempts, a DNA product was not obtained from three bone samples for both HVI and HVII. These included petrous portions from individuals 1241 and 5075, and a tibia from individual 1225. Various other bone samples generated a PCR product for one of the hypervariable regions, but not the other. HVI could not be amplified from a fibula sample from individual 5010 or a humerus from 1518. Skull petrous portions from individuals 5043 and 3023 did not give an HVII amplification product, nor did a fibula from 5189, a femur from individual 1259, and an ulna from 1226.

Table 3: Drilling and Amplification of Bone Types

Types of bones utilized for DNA analysis and the number of each that could be successfully drilled and DNA amplified. Bones were drilled successfully when at least 20 mg of bone powder was obtained. Skeletal sample types are broken down into three age categories; adult, subadult, and infant.

Skeletal Sample	Drilling Attempted	Drilled Successfully	HVI Amplification	HVII Amplification
Fibula (adult)	5	5	3	5
Fibula (subadult)	4	3	3	2
Fibula (infant)	2	0	0	0
Humerus (adult)	3	3	2	3
Humerus (subadult)	2	2	2	2
Humerus (infant)	1	1	1	1
Radius (adult)	1	1	1	1
Radius (subadult)	0	0	0	0
Radius (infant)	0	0	0	0
Petrous portion (adult)	1	1	1	0
Petrous portion (subadult)	6	6	5	5
Petrous portion (infant)	11	10	8	8
Tibia (adult)	0	0	0	0
Tibia (subadult)	2	2	1	1
Tibia (infant)	4	3	3	3
Ulna (adult)	2	2	2	1
Ulna (subadult)	0	0	0	0
Ulna (infant)	2	2	2	2
Femur (adult)	1	1	1	1
Femur (subadult)	3	3	3	1
Femur (infant)	2	2	2	2
Rib (adult)	0	0	0	0
Rib (subadult)	1	1	1	1
Rib (infant)	1	0	0	0
Clavicle (adult)	0	0	0	0
Clavicle (subadult)	0	0	0	0
Clavicle (infant)	1	0	0	0
Skull Frontal frag. (adult)	0	0	0	0
Skull Frontal frag. (subadult)	0	0	0	0
Skull Frontal frag. (infant)	1	1	1	1
Unknown (adult)	0	0	0	0
Unknown (subadult)	2	2	2	2
Unknown (infant)	0	0	0	0

MtDNA Sequencing

HVI and HVII sequences obtained from bone samples as well as consensus sequences for individuals are detailed in Tables 10 through 13. Sequencing was conducted on any sample that gave sufficient amplification product. In most cases, sequencing attempts resulted in analyzable results, although several could not be analyzed due to too little or too much DNA template or the presence of sequencing artifacts. When successful amplification of both a DNA sample and the dilution occurred, PCR product from the 1:20 dilution was also analyzed to confirm the data generated. Samples that produced no analyzable data due to capillary failure or other problems such as not enough or too much template were re-sequenced. Some sequences were difficult to analyze because of various artifacts including pull-up and extra peaks that appeared consistently throughout the sequence (Figure 7). Approximately 150 to 200 base pairs of sequence were obtained from each hypervariable region (Table 4).

Figure 7: Sequencing Artifacts

Two sequencing artifacts commonly witnessed in electropherograms were extra peaks and pull-up peaks. Extra peaks (A) increased the number of ambiguous positions observed in sequences, while bases called by the software as a result of pull-up peaks (B) were easily recognized and removed. Sequencing artifacts are designated by arrows.

A. Extra Peaks

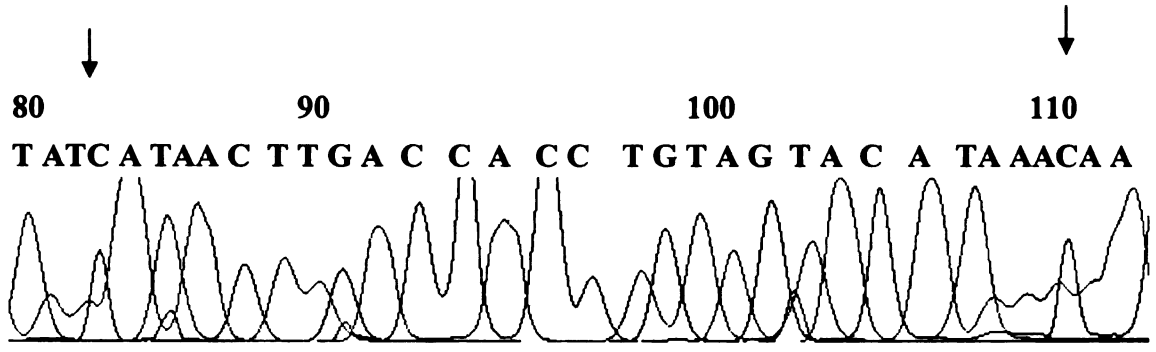

B. Pull-up

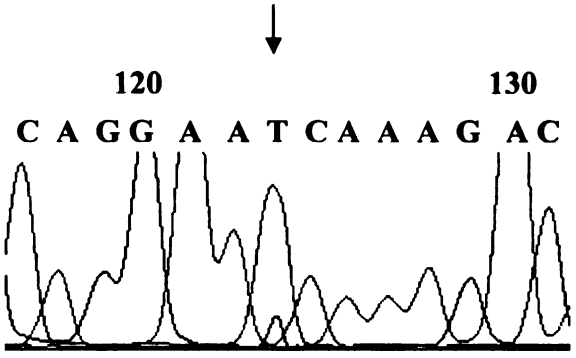

Table 4: Regions of Sequence

Regions of sequence obtained from each bone are shown for both HVI and HVII. Sequence regions obtained refer to areas of mtDNA sequence that were analyzable using BioEdit software. The total number of analyzable bases from HVI and HVII combined is also provided.

Burial	Bone Type	HV1 Sequence Region Obtained	HVII Sequence Region Obtained	Number of Bases
1185	fibula shaft	16060 – 16207	21 – 205	331
1187	right radius midshaft	15990 – 16199	16 – 284	477
1187	right fibula midshaft	16061 – 16173	93 – 275	294
1188	left humerus shaft	16060 – 16204	18 – 233	359
1188	right petrous portion	16061 – 16169	94 – 284	298
1224	left petrous portion	16061 – 16208	103 – 235	279
1224	right humerus midshaft	16060 – 16205	112 – 284	317
1225	right petrous portion	16059 – 16150	95 – 228	224
1225	left tibia midshaft	None	None	0
1226	right fibula	16062 – 16198	92 – 281	325
1226	left ulna midshaft	16069 – 16204	None	135
1229	left petrous portion	None	None	0
1229	humeral shaft	16063 – 16205	160 – 284	266
1259	left femur midshaft	16062 – 16203	None	141
1264	tibia cortical fragment	16063 – 16197	95 – 251	290
1264	fibula midshaft	16069 – 16194	107 – 267	285
1236	fibula midshaft	16059 – 16203	88 – 278	334
1236	left ulna midshaft	16061 – 16208	91 – 187, 197 – 277	323
1241	right petrous portion	None	None	0
1241	fibula midshaft	None	None	0
1267	petrous portion	16083 – 16203	91 – 284	313
1267	tibia fragment	None	None	0
5043	right petrous portion	16069 – 16203	None	134
5043	fibula midshaft	None	None	0
5075	left petrous portion	None	None	0
5075	right rib	None	None	0
5111	left petrous portion	16063 – 16203	93 – 289	336
5111	femur midshaft	16062 – 16210	95 – 282	335
5189	fibula midshaft	16060 – 16208	None	148
5628	r. petrous portion	16064 – 16187	153 – 279	249
5268	r. femur fragments	16069 – 16203	109 – 251	276
5641	right petrous portion	16062 – 16202	85 – 267	322
1452	l. femur fragment	16062 – 16200	91 – 274	321
1456	r. petrous portion	16070 – 16212	97 – 268	313
1456	r. clavicle	None	None	0
3122	r. tibia	16057 – 16207	93 – 223	280
3122	frontal fragment	16086 – 16193	107 – 274	274

Table 4 (continued)

Burial	Bone Type	HV1 Sequence Region Obtained	HVII Sequence Region Obtained	Number of Bases
3126	l. petrous portion	16065 – 16205	102 – 284	322
3126	fibula fragment	None	None	0
1502	left ulna	16066 – 16209	109 – 249	283
1502	tibia	16059 -16195	103 – 282	315
1517	right petrous portion	16064 – 16203	86 – 266	319
1517	right ulna	16059 – 16205	94 – 274	326
1518	humeral cortical frag	None	85 – 279	194
1518	humeral cortical frag	16062 – 16202	92 – 228	276
1518	fibula midshaft	None	105 – 279	174
5010	fibula midshaft	None	85 – 284	199
5010	humerus midshaft	16061 – 16205	95 – 279	328
1406	l. petrous portion	None	124 – 285	161
1406	l. femur	16096 – 16195	None	99
1548	r. petrous portion	16056 – 16184	92 – 279	315
1548	l. tibia	16067 – 16205	89 – 277	326
3018	petrous portion	16094 – 16204	96 – 274	288
3018	rib	16055 – 16205	92 – 274	332
3023	petrous portion	16087 – 16175	None	88
3023	femur	16080 – 16202	96 – 284	310
3060	Unknown	16062 – 16198	None	136
3060	Unknown	16061 – 16208	92 – 283	338

Sequence Ambiguities

Many of the sequences generated from the bone samples contained at least one ambiguity in which a clean base call could not be made. Although additional sequencing attempts were made to try to discern which base was present at ambiguous positions, a call could not always be made. In HVI, 65% of the sequences generated from individual bone samples contained at least one ambiguity. When HVI sequences obtained from all bones for an individual were combined to create a consensus sequence, 71% of the consensus sequences contained at least one ambiguous position. The HVII sequences, which were approximately 50 base pairs longer, contained a slightly higher number of

ambiguities; 34 of the 41 (83%) sequences obtained from individual bones contained at least one ambiguous position, while 81% of the consensus sequences had at least one.

Ambiguities in sequences presented in three different ways. At times, forward and reverse sequences showed discrepancies at certain positions. The ambiguous bases of this type were able to be called with confidence later on based on sequences that were generated from other sequencing attempts. In addition, conflicting bases occurred at a specific position in two or three bones from one individual. Finally, some ambiguous positions were consistent in more than one bone from an individual. This occurred in the HVI sequence of individual 1236 with all bones generating a W at position 16199.

Several of the ambiguous positions observed in multiple bones were also seen in other individuals, as was the case for 4 positions in HVI and 14 positions in HVII. When ambiguities were present, they tended to occur at one of several "hotspots" along the sequence (Table 5). In HVI, multiple ambiguities were present at positions 16093, 16124, 16189, and 16199 (Table 5). HVII contained a larger number of common ambiguities, at positions 146, 150, 152, 153, 158, 159, 187, 195, 199, 204, 225, 226, 267, and 280. One pattern that was noted among the HVII hotspots was at positions 158 and 159. This ambiguity was present at both positions and never only 158 or 159. This trend was observed in 6 of the sequences from single bones but was not present in consensus sequences.

Table 5: Ambiguity Hotspots

Ambiguous positions that were noted in more than one individual. Each position in relation to the Cambridge Reference Sequence is listed as well as how many individuals displayed an ambiguous base at that position.

Position	# Individuals with Ambiguities
146	2
150	8
152	5
153	4
158 and 159	6
187	4
195	10
199	6
204	4
225	4
226	3
267	4
280	7
16093	4
16124	3
16129	4
16189	6
16199	12

The types of ambiguities occurred in differing frequencies. In total, 57 ambiguous bases were present in the sequence data within HVI while the number of ambiguous bases present in HVII was much greater (81). Once multiple bone sequences were combined to create a consensus sequence, the number of ambiguities decreased to 16 and 28 for HVI and HVII, respectively. The frequency of certain ambiguities varied from HVI to HVII, as well as when comparing individual sequences versus consensus sequences. The most common type of ambiguity in HVI was a W (an A or T), followed by M (A or C), and Y (C or T). The pattern changed in the consensus sequences as the most commonly observed ambiguities in HVI were Y and W. Y was the most frequent

ambiguity in HVII sequences, followed by M (Table 6). In consensus sequences, Y was still seen the most, although the number of R ambiguities (A or G) was common as well.

Table 6: Frequency of Ambiguities in HVI and HVII MtDNA Sequences

Ambiguities observed in sequences are listed as well as the number of each ambiguity in HVI and HVII consensus sequences for individuals.

Ambiguity	Number of Times Observed in HVI	Number of Times Observed in HVII
Y	7	14
W	7	0
M	0	3
R	1	10
K	0	1
H	1	0
S	0	0
N	0	0

MtDNA Haplotypes

In all, nine haplotypes were present among the burials in this study. Preliminary haplotypes including ambiguities are detailed in Tables 7 and 8. The majority of consensus sequences contained ambiguous positions with no informative polymorphisms. When ambiguous bases were omitted from the sequences, the haplotypes were not found to be different from the CRS with the exception of position 263G, which is a common polymorphism in Europeans and is therefore not useful in differentiating individuals. The resultant "undifferentiated" haplotype was designated haplotype 1. Haplotypes 2 through 9 all contained at least one distinctive polymorphism that differed from the CRS and from each other. Haplotype 2 was assigned to individuals whose sequence was marked by a T at position 150 in addition to 263G polymorphism. Haplotype 3 contained

a C at position 199, a C at position 204, and 263 G. Haplotypes 1 through 3 occurred in more than one individual, while 4 through 9 were unique.

Table 7: HVI Haplotypes Including Ambiguities

Fifteen haplotypes within HVI were designated for all burials (A). Haplotypes are defined by differences from the Cambridge Reference Sequence. HVI mtDNA consensus haplotype determined for each burial by room are displayed (B). Haplotypes include ambiguities present within sequences.

A.

Haplotype	Differences from CRS
HV1-1	Anderson
HV1-2	16080W
HV1-3	16129R
HV1-4	16198W
HV1-5	16189Y
HV1-6	16199W
HV1-7	16189Y, 16199W
HV1-8	16187M, 16199W
HV1-9	16093Y, 16199W
HV1-10	16093K, 16126C, 16133T, 16145A, 16199W
HV1-11	16087M, 16164W, 16179S
HV1-12	16124Y, 16135W, 16138W, 16148M, 16149M, 16150M
HV1-13	16126C, 16163G, 16186T, 16189C, 16199A
HV1-14	16102K, 16106R, 16124C, 16144K, 16189K
HV1-15	16124Y, 16126Y, 16146R

Table 7 (continued): HVI Haplotypes Including Ambiguities

Fifteen haplotypes within HVI were designated for all burials (A). Haplotypes are defined by differences from the Cambridge Reference Sequence. HVI mtDNA consensus haplotype determined for each burial by room are displayed (B). Haplotypes include ambiguities present within sequences.

B.

Room	Burial	Haplotype
N	1188	HV1-9
	1187/1189	HV1-1
	1224	HV1-6
	1225	HV1-12
	1226	HV1-1
	1229	HV1-3
	1259	HV1-6
	1264	HV1-5
	1267	HV1-10
	1185	HV1-6
O East	1236	HV1-9
	1241	no seq. data
	5043	HV1-4
O West	5010	HV1-8
	5075	no seq. data
	5111	HV1-6
	5189	HV1-13
	1406	HV1-14
V	1548	HV1-1
T/U	1518	HV1-1
	1502	HV1-1
	1517	HV1-9
Q	5641	HV1-2
	5268/5631	HV1-3
S	1456	HV1-6
	3126	HV1-11
	3122	HV1-5
	1452	HV1-15
MH	3018	HV1-7
	3023	HV1-7
	3060	HV1-1

Table 8: HVII Haplotypes Including Ambiguities

Twelve haplotypes within HVII were designated for all burials (A). Haplotypes are defined by differences from the Cambridge Reference Sequence. HVI mtDNA consensus haplotype determined for each burial by room are displayed (B). Haplotypes include ambiguities present within sequences.

A.

Haplotype	Differences from CRS
HVII-1	198Y
HVII-2	263G
HVII-3	152Y, 263G
HVII-4	187R, 263G
HVII-5	150T, 195Y, 263G
HVII-6	150T, 195Y, 200R, 263G
HVII-7	153R, 195Y, 225R, 226Y, 263G
HVII-8	150Y, 153R, 195Y, 225R, 227R, 263G
HVII-9	150T, 152C, 195Y, 225R, 226Y, 240M, 263G
HVII-10	199C, 204C, 263G
HVII-11	185R, 228R, 234M, 263G
HVII-12	195Y, 199Y, 225R, 226Y, 263G
HVII-13	146C, 152C, 195C, 263G
HVII-14	95M, 111M, 116M, 139K, 155K, 263G
HVII-15	134W, 146Y, 186M, 187R, 263G

Table 8 (continued): HVII Haplotypes Including Ambiguities

Twelve haplotypes within HVII were designated for all burials (A). Haplotypes are defined by differences from the Cambridge Reference Sequence. HVI mtDNA consensus haplotype determined for each burial by room are displayed (B). Haplotypes include ambiguities present within sequences.

B.

Room	Burial	Haplotype
N	1188	HVII-5
	1187/1189	HVII-2
	1224	HVII-5
	1225	HVII-10
	1226	HVII-10
	1229	HVII-2
	1259	no seq. data
	1264	HVII-2
	1267	HVII-14
	1185	HVII-1
O East	1236	HVII-7
	1241	no seq. data
	5043	no seq. data
O West	5010	HVII-5
	5075	no seq. data
	5111	HVII-8
	5189	no seq. data
	1406	HVII-2
V	1548	HVII-13
T/U	1518	HVII-12
	1502	HVII-11
	1517	HVII-6
Q	5641	HVII-2
	5268/5631	HVII-9
S	1456	HVII-4
	3126	HVII-2
	3122	HVII-3
	1452	HVII-15
MH	3018	HVII-2
	3023	HVII-2
	3060	HVII-2

In total, sequences were obtained from 29 of the 31 individuals analyzed. No sequence data could be generated for burials 5075 and 1241. A complete listing of assigned haplotypes can be found in Table 9. Seventeen of the individuals typed had undifferentiated sequences and were assigned haplotype 1. Haplotype 2 was shared by individuals 1188, 1224, 5010, and 1517. Haplotype 3 was shared by individuals 1225 and 1226. The remaining haplotypes (4 through 9) were assigned to burials 5268, 1267, 1406, 5189, 1548, and 1452, respectively. A spatial analysis of haplotypes within the palace and Merchant's House was performed to determine the locations and distribution of each (Figure 8). This analysis revealed that individuals who shared haplotype 2 or 3 were located near one other individual, while most individuals with unique haplotypes were in a different directional orientation, or located away from other burials.

Table 9: Haplotype Designations

Nine haplotypes were assigned when ambiguities within sequences were not included (A). Haplotypes assigned to burials by room as well as the biological profile for each burial are provided (B). Haplotypes include HVI and HVII.

A.

Haplotype Designation	Differences from CRS
1	Undetermined (263G)
2	150T, 263G
3	199C, 204C, 263G
4	150T, 152C, 263G
5	16126C, 16133T, 16145A
6	263G, 16124C
7	16126C, 16163G, 16186T, 16189C, 16199A
8	146C, 152C, 195C, 263G
9	146C, 263G

Table 9 (continued): Haplotype Designations

Nine haplotypes were assigned when ambiguities within sequences were not included (A). Haplotypes assigned to burials by room as well as the biological profile for each burial are provided (B). Haplotypes include HVI and HVII.

B.

Room	Burial	Sex, Age	Haplotype
N	1188	11 – 13 yrs	2
	1187/1189	Male, 30 – 45 yrs	1
	1224	3 – 4 yrs	2
	1225	3 – 4 yrs	3
	1226	Male, 35 – 45 yrs	3
	1229	3 – 6 mos	1
	1259	10 – 12 yrs	1
	1264	6 – 8 yrs	1
	1267	34 wk fetus	5
	1185	adult	1
O East	1236	Female, 23 – 27 yrs	1
	1241	3 – 9 mos	no sequence data
	5043	1 – 2 yrs	1
O West	5010	Female, 35 – 45 yrs	2
	5075	0 – 2 mos	no sequence data
	5111	6 mos	1
	5189	12 – 15 yrs	7
V	1406	3.5 – 4.5 yrs	6
	1548	neonate	8
T/U	1518	Male, 40+ yrs	1
	1502	6 mos – 1 yr	1
	1517	6 mos	2
Q	5641	Late fetal – birth	1
	5268/5631	3 – 5 yrs	4
S	1456	neonate	1
	3126	6 mos	1
	3122	6 mos – 1 yr	1
	1452	3 – 6 mos	9
MH	3018	12 – 14 yrs	1
	3023	Male, 25 – 35 yrs	1
	3060	13 – 15 yrs	1

Figure 8: Haplotype Distribution

Locations of each burial within the Triconch Palace or Merchant's House are pictured. Burials for which a haplotype was determined are designated by a number in parentheses next to the burial number. Each number represents a haplotype (1 – 9).

Figure 8: Haplotype Distribution

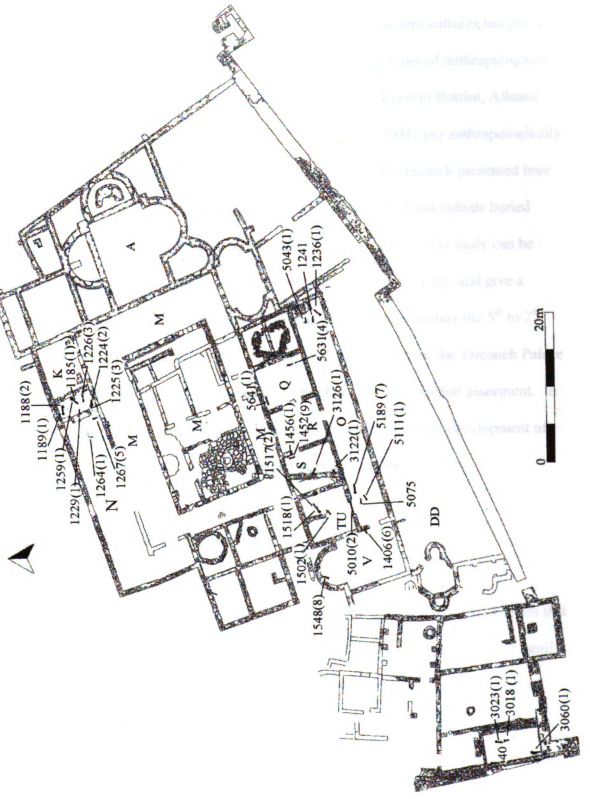

Discussion

The application of molecular techniques to studies of ancient cultures has proven to be a valuable tool in partnership with other more traditional types of anthropological analyses. The Triconch Palace and the adjacent Merchant's House in Butrint, Albania have been well characterized archaeologically (Hodges et al. 2004) and anthropologically (Fenton, personal communication). The mtDNA analysis in the research presented here provides unique insights pertaining to the familial relationships of individuals buried within the Palace and Merchant's House. In addition, the data from this study can be used to infer burial systems, demographic information, genetic diversity, and give a larger picture of what life may have been like in Butrint in approximately the 5th to 7th and 13th to 15th centuries. The mtDNA haplotypes obtained for 29 of the Triconch Palace burials shed light on the relationship between individuals and their spatial placement. In addition, the observations made during this research may aid in further development of protocols and techniques for processing ancient skeletal material.

The Triconch Palace and Merchant's House as a Burial Site

Archaeological and anthropological evidence exists supporting the hypothesis that clusters of burials located within the Triconch Palace and Merchant's House were family units. Many of the burials in each grouping share an east to west orientation. This is consistent with the predominance of Christianity in the area at the time as it is Christian tradition to bury individuals in this manner (Rose 1922). In addition, biological profiles of clustered burials fit the framework of a family. In each grouping, one to three adults

were present along with several subadults of various ages. For example, the cluster located near room O west contained an adult male, an adult female, and six subadults, thus the anthropological profile alone suggests that this may have been a family unit.

Molecular data from this study strengthen the hypothesis that the Triconch Palace was used by families as a place to bury their dead, as individuals with shared haplotypes 2 and 3 were present in two clusters. The two haplotype 3 individuals located in the room N cluster (1225 and 1226) were a subadult and an adult male, and may represent siblings, or could have a different type of maternal relationship such as cousins or an uncle and nephew or niece. If the latter is the case, the groupings included extended family rather than just nuclear family members. The four individuals sharing haplotype 2, located in pairs in the room N and room O west clusters, complicate matters somewhat. 1188 and 1224 (both subadults), although located in room N, were not buried next to one another but instead were along opposite walls of the room. Likewise, 5010 (adult female) and 1517 (subadult), in room O, were buried on different sides of the cluster. The fact that all individuals with haplotype 2 were not located within one cluster and were not situated next to each other, but rather were across a room, seems inconsistent with burying family members together. There are multiple potential explanations that help to make sense of this inconsistency however. If the groupings included extended family members dispersed among nuclear family members, it would not necessarily be the case that maternal relatives were buried next to one another. In addition, if family members died and were buried at different times, it may have proven difficult to pinpoint where the earlier burial was located, making it impossible to bury two family members directly next

to each other. Finally, haplotype 2 was found in four individuals, so it may have been common in the population and present in two separate maternal lines.

The prevalence of haplotype 1 in the Triconch Palace provides additional support for the hypothesis that clusters represent family burials. It seems quite likely that some individuals with haplotype 1 were indeed maternally related, although it is impossible to determine from the data due to the lack of informative polymorphisms and the large number of individuals of haplotype 1. Had the haplotype been very rare (from a modern perspective), the presence of many individuals with haplotype 1 would strengthen the hypothesis that clusters were family members and would also indicate that one maternal lineage was predominantly using the Triconch Palace as a burial site. It is more likely however, that haplotype 1 was common within the population overall (as it is today), and therefore provides little information about the number of families present in the Triconch Palace.

One somewhat unexpected finding was the large proportion of spatially separated individuals within the Triconch Palace having unique haplotypes (haplotypes 4 through 9), which is seemingly inconsistent with the use of the site as a familial burial plot. Similar to those with shared haplotypes, these burials were present in interesting patterns. Five of the six individuals with unique haplotypes were buried on the south side of the Palace in the rooms closest to the Vivari Channel. Five of six were also distinct from the clusters of individuals, being either separate from other burials, or not found in an east-west orientation. Individuals with unique haplotypes, including 5268 (3 to 5 year old), 1267 (fetus), 1548 (fetus), and 1452 (3 to 6 months) were positioned in a north-south direction, and burial 1406 (3.5 to 4.5 years) was located alone in room V of the Palace.

One explanation for the unexpected number of unique haplotypes is that a diverse group of people was using the Triconch Palace as a burial area. This would have been the case if the resident Butrint population itself was diverse, or if people from outside the area were occasionally burying individuals at the site. The latter seems to be more likely because of the commonality of haplotype 1 and its spatial location within the Palace, with the haplotype being distributed evenly among the clustered burials, but not present among those that were isolated. If the unique haplotypes resulted from a genetically diverse resident population, they would most likely be distributed more evenly throughout the Triconch Palace. Instead, their location along the Vivari Channel strengthens the idea that people traveling through Butrint buried the individuals, as access to the Palace from the waterway would have been fairly easy. Prior to the 5th century, Butrint was an important port along an active trade route. This, combined with the predominant fishing industry, made travel through the Vivari Channel commonplace. Based on the frequent use of the waterway, as well as the north-south orientation of the burials, it is possible that people continued to pass through Butrint via the channel and buried their dead in what had become a cemetery in the Triconch Palace, but separate from burial clusters.

The large proportion of unique haplotype burials that were very young children indicates that they may have been part of some form of a child cemetery. This type of cemetery, which was present in other Mediterranean areas at the time, was one in which people generally buried only infants (Derevenski 2000). Although it is possible the burials were part of a dedicated child cemetery, it seems unlikely because not all of the five sets of remains had an age consistent with a child cemetery, as the sixth was 12 to 15

years old. Further, the burials were not spatially grouped close together. If a child cemetery had been present in the Palace, one would expect, based on other child cemeteries (Soren et al.1995, Derevenski 2000), the burials to be located near each other, not spread out, and that all individuals would be very young children.

The presence of individuals with shared haplotypes in the Triconch Palace, as well as those with unique haplotypes in different locations, prompts a more complex explanation for the burial patterns, as opposed to the original hypothesis that it was used solely for family burials. An interesting possibility is that the Palace was utilized as a burial site in more than one way. The shared haplotypes and clusters of burials in similar orientations is consistent with the use of the Triconch Palace by several families as a burial ground. If the unique haplotypes are not considered, at least three maternal lines were buried there, haplotypes 1, 2, and 3. At the same time however, it seems likely that unrelated individuals were being interred by people from outside the area passing through the Vivari Channel. Another interesting consideration is that the burials in the Palace were originally dated from the 5^{th} to 7^{th} centuries by archeologists at the site. Their more recent estimates are that instead, these burials occurred over a period of years or decades (Fenton, personal communication). This time period is consistent with the use of the site by both families and individuals passing through Butrint, as individuals in the clusters, including adults, indicates that only one or two generations were buried in each grouping. The number of burials distinct from the clusters, those with unique haplotypes, was also low, again indicating interment over shorter periods of times. If travelers had used the Triconch Palace over an extended time frame, more burials with unique haplotypes would be expected.

Given the genetic data from the Triconch Palace and Merchant's House, some general information about the society of Butrint during this time period can be deduced, which support previous archaeological findings indicating there was a drastic decline in human occupation of the area, and that the city was in decay. Several of the skeletal remains showed pathologies (Fenton, personal communication). For example, remains from individuals 3018 and 3060 had vertebral lesions indicative of long-term bacterial infections, which were shown to result from brucellosis (Mutolo 2006). In addition, porotic hyperostosis was present in remains from 5631, which is an indicator of anemia, recognizable in skeletal material by the presence of small holes on the outer surface of the skull. Anthropological evidence of disease is consistent with a high mortality rate in Butrint. The large proportion of subadult burials, particularly the very young, suggests that infant mortality was particularly high. Another indication of difficult times is the change that occurred in burial patterns. The transition from burials outside the city to burial inside the Palace itself supports the archaeological hypothesis that Butrint was a city in flux. A shift in a fundamental value of a society, such as how and where the dead are interred, suggests that Butrint was no longer a thriving trade center and that people's way of life had been altered. The hypothesis that Butrint had changed and was a city in decay rather than a populated center of commerce is consistent with people from outside the city passing through the Vivari Channel and burying a dead child. If Butrint was still thriving, the interior of the city would not be an attractive place to bury an individual.

Genetic Implications of Haplotype Distributions

Genetic inferences can be made about the population inhabiting Butrint based on the number of haplotypes observed in the 29 burials, as well as the number of individuals that shared haplotypes. The finding that haplotype 1 was shared by over half the burials is consistent with certain attributes of a population, including loss of genetic variation resulting from the profound effects of genetic drift on very small populations, or a founder effect, in which very few individuals settled in the area, resulting in a population with low genetic diversity. In such a small population, inbreeding would be increasingly likely, once again lowering genetic variation. It is interesting to note that haplotype 1 was also seen in the burials from the Merchant's House, interred hundreds of year later. The persistence of the haplotype through several centuries indicates that there was not a large increase in genetic diversity over time by new lineages settling in the area. Overall, the decay of Butrint and population decline was likely to have had a profound effect on not only the social customs of the people, including burial traditions, but also the genetic makeup of those in the area.

DNA Analysis Utilizing Ancient Skeletal Remains

The work on the ancient skeletal remains found in Butrint presented unique challenges that led to new insights and protocols for processing them for DNA analysis. The age of the remains combined with the small size of many of the bones prompted modifications to techniques used in previous studies of ancient burial sites (Misner 2004,

Rennick 2005, Murray 2006, Mutolo 2006). Difficulties were encountered while preparing bones for DNA analysis, particularly because almost all of the skeletal samples contained a large amount of soil. Although the outside surface of many of the bones appeared to be clean, and any obvious debris was removed by swabbing with water or bone wash, once drilling commenced the vibrations dislodged small amounts of soil present on the surface or in the interior of the bone, causing it to fall into the powder being collected. This was particularly evident in bones that contained crevices or whole long bones in which bone marrow had been replaced by soil. Skull petrous portions were especially troublesome because of the many small crevices on the surface. For most bones, extra soil resulted in darker extracts and likely contributed to PCR inhibition due to substances known to be in soil, such as humic acid, which have been found to be inhibitory at concentrations as low as 10 ng in a 100 μL PCR reaction (Tsai and Olsen 1992).

The prevalence of soil encountered in the skeletal samples, in combination with increased difficulty of collecting pure bone powder, led to the development of an extra cleaning step prior to drilling. Instead of using swabs, water, and bone wash to remove soil, skeletal samples were flushed with water and scrubbed gently with a glassware brush to remove soil from crevices on the bone surface. The bones were allowed to dry overnight and any soil still visible was removed by swabbing with water and bone wash. This more rigorous cleaning made the drilling process much easier, especially for samples such as skull petrous portions, and resulted in the collection of cleaner bone powder and less colored extracts.

Previous research indicated that certain bone types yield more amplifiable DNA of higher quantity and quality. Misner (2004) suggested that femur be used for DNA sampling rather than flat bones such as pelvis or rib because it gave a higher rate of DNA amplification. She concluded that this is because the lower surface area to volume ratio of long bones such as femur and the larger cortical layer provide a greater area of protected DNA. Murray (2006) recommended that petrous portion also be utilized because it had a higher rate of DNA amplification than long bones (67% overall versus approximately 50%). Both femur and petrous portion were observed to contain more cortical bone than other skeletal material, which was hypothesized to provide more protection for cells or DNA itself. In the current study femur and petrous portions were easier to drill because of their inherent strength. Typically, larger long bones had a better surface for drilling if the samples were cut at 90 degrees to the length of the shaft. This revealed the cortical bone that could be easily drilled if it was sufficiently thick. Petrous portions were generally more challenging to drill because of their hardness as well as the irregular surface and crevices internally present in the bone.

This study presented a unique challenge due to the large number of skeletal samples from children. Of the 31 burials analyzed, 77% were children, with 42% being infants. The small size and frailty of many of the bones made collecting powder extremely difficult or impossible. This was especially true of long bones from children because powder could not be obtained by drilling into the bone shaft as was done for adult samples. Several were so fragile that they could not even be adequately cleaned prior to processing. In many instances, powder had to be collected through sanding or grinding the surface of the bone shaft. In samples where the cortical bone layer was very

thin, the interior of the bone often became exposed, along with the soil harbored inside. Owing to this, the bone type of preference for sampling young children and infants was the petrous portion. Despite the small size of bones from children in general, these were often large enough to drill easily, and sufficient bone powder was generated from all but one of the petrous portions available. For these reasons the petrous portion was the bone type used most frequently for children, as well as across all age groups.

The bone types from which DNA amplified most frequently were comparable to those in previous studies of ancient skeletal samples in the MSU Forensic Biology Laboratory (Misner 2004, Rennick 2005, Murray 2006). Fibula, radius, humerus, and ulna did not require nested PCR as frequently as did other bones, although more samples would be needed to make any conclusions, as less than 10 of each were analyzed. After nested PCR, most skeletal samples had similar amplification success, with radius, rib, and frontal portion of the skull all having the highest amplification rates (100%) (Table 3). Bone types that were sampled more frequently (petrous portion, fibula, humerus, and femur) had similar DNA amplification rates of roughly 85%, which differed slightly from those seen by previous researchers in the laboratory. Rennick (2005) reported that DNA from femur, petrous portion, and humerus had the highest amplification percentages (92%, 90%, and 81% respectively). Murray (2006) found that petrous portion DNA amplified 67% of the time, followed by humerus (59%) and femur (50%). The bone samples in those studies dated to between the 13th and 6th centuries B.C., thus the different overall amplification success may be explained by varying environmental conditions in each area as well as age of the remains. Findings by Edson et al. (2004) of the Armed Forces DNA Identification Laboratory were also similar to what was found in

this study. The authors suggested that long bones, especially those that are weight-bearing, give the highest DNA amplification rates, and that femur should be chosen for analysis if possible. Interestingly, Edson et al. (2004) found that cranial bones had the lowest DNA amplification success rate, but did not specifically look at the petrous portions. Currently, AFDIL is beginning to use petrous portions for DNA analysis based on studies conducted by the MSU Forensic Biology Laboratory (Foran, personal communication).

The sensitivity of PCR allows for the amplification of extremely small amounts of DNA. In theory, a single template strand may be amplified to create DNA sufficient for analyses. PCR is essential in molecular analysis of ancient samples because the quantity and quality of starting DNA is generally very limited. Unfortunately, the ability to amplify small amounts of template also allows for amplification of any exogenous DNA that may be present. Contamination can originate from various sources if the proper precautions are not taken, including researchers that handled bones at any point, reagents, tubes and other materials, as well as carry-over from previous PCR amplifications or high quantity DNA sources. Numerous steps were taken to reduce the risk of contamination from each of these. All post-amplification procedures were carried out in a dedicated PCR laboratory separated from the laboratory in which DNA sampling, extraction, and PCR set-up occurred. Personal protective equipment, including disposable mask, sleeves, and latex gloves was worn to minimize contamination introduced by the researcher, especially during pre-amplification procedures. Drilling and DNA extractions were performed in a UV-sterilized hood and if multiple bones from an individual were analyzed, they were processed on different days. Protocols for drilling included steps to

remove any exogenous DNA contaminating the surface of the skeletal sample to ensure that DNA sequences obtained were endogenous to the bone and not from other sources. Reagent blanks and negative controls were used throughout the research to ensure that no DNA contamination was present in reagents and to verify that the source of any DNA contamination was not the researcher.

Despite stringent precautions, contamination was observed on multiple occasions, both in reagent blanks and in negative controls, though often not at the same time and not in both HVI and HVII amplifications carried out side-by-side. In order to track contamination sources, any reagent blanks and negative controls that gave an amplification product were sequenced and compared to the mtDNA sequence of the researcher as well as to sequences obtained for bone samples. When the contaminating sequence was consistent with the researcher or was a sequence also obtained from a bone sample, a new PCR was set up using new reagents, while DNA was re-extracted from the bone if contamination was present in the extraction blank. If bone sequences were that of the researcher, they were not included in the results. Successful attempts were made to reduce contamination of unknown origin by using fewer cycles for amplification in the nested PCR, as this was the step after which contamination was observed. Possible sources of contaminating DNA were microcentrifuge tubes or PCR tubes utilized during extraction and PCR, although materials were UV irradiated prior to use. Another potential source was reagents used that could not be UV irradiated such as Taq polymerase or primers. If a small amount of template was present in these reagents, it may have been distributed stochastically to some reactions but not others.

An additional problem encountered in DNA analysis of the remains was the presence of ambiguous bases in mtDNA sequences, most likely due to DNA degradation. Post-mortem mutation is frequently observed in ancient skeletal samples (Hofreiter et al. 2001). Chemical modifications can cause bases to change structure and as a result, a different base can be incorporated into a DNA strand over the course of PCR. Typically, DNA degrades continuously through processes such as hydrolysis and oxidation (O'Rourke et al. 2000). Post-mortem base modifications that occur in one DNA strand are not remedied by nucleotide excision repair mechanisms as they would be if an organism was still living. These mutations often result in the observance of an ambiguous base once the DNA is sequenced.

Post-mortem mutation is a likely explanation for the large number of ambiguities present in the sequences generated during the course of this study (see Results). According to Hofreiter et al. (2001), the post-mortem mutation that occurs most frequently is a C to T transition. This is a result of deamination of cytosine to uracil, causing a complementary thymine to be incorporated by the polymerase during PCR. If the opposite strand is sequenced, this is read as a G to A transition. The most common ambiguity in the Triconch Palace samples across HVI and HVII, as well as when comparing individual bones and consensus sequences, was a C or T. Ambiguous positions at which a G or an A was present were the second most common in consensus sequences.

Several other sequence ambiguities were also observed. HVI contained a number of T or A ambiguities, equivalent to the quantity of C or T calls. Over half of the T or A ambiguities observed in individual bone sequences and 5 of the 7 in consensus sequences

were present at position 16199. The ambiguities appearing as either an A or C in HVI were usually present only in sequences obtained from one bone and were not found once consensus sequences were determined. Patterns were observed in its occurrence that suggest it could result from sequencing artifacts (discussed below).

As the postmortem interval increases, mutations accumulate, therefore sequences from older skeletal remains should contain a greater number of ambiguities. This was observed in sequences from individuals buried within the Triconch Palace from the 5th to 7th centuries as compared to the three Merchant's House individuals from the 13th to 15th centuries. Very few ambiguous positions were present in sequences from the remains buried eight centuries later, and those observed were the more common C or T ambiguities.

An alternative explanation for ambiguous base calls is heteroplasmy, which has been found in mtDNA of various tissue types including blood, buccal cells, and hair roots (e.g., Bendall et al. 1997). Heteroplasmy occurs when an individual contains two different nucleotides at a mtDNA position, and is present while an individual is alive as well as post-mortem. Although heteroplasmy has been reported in several tissues, it has not been extensively studied in skeletal samples (Bendall et al. 1997, Theves et al. 2006). Heteroplasmy is fairly uncommon, typically only occurs at one position, and is very rarely observed at multiple places in a sequence (Budowle et al. 2002). The frequent occurrence of ambiguities in the sequence data from this study, as well as the observation of multiple ambiguities within a sequence, indicate that the ambiguities in the mtDNA sequences of the Triconch Palace individuals are due to post-mortem mutation rather than heteroplasmy.

In all cases where a sample was successfully amplified and the resulting DNA was carried through sequencing protocols, a sequence was obtained. Forward and reverse sequencing reactions were performed for each amplicon, and when available, a PCR product of a sample dilution was sequenced along with the PCR product obtained from the full concentration extract. This generated multiple strands of sequence to align and aid in making base call confirmations. Not all samples produced multiple analyzable sequences, however. Difficulties occasionally occurred in sequencing reactions, including addition of too much or too little template, which could be diagnosed by examining the relative fluorescent unit value of the CEQ 8000 signal output. In those instances the sample was reinjected for a shorter or longer time. Further, some sequences were "messy" and challenging to align and analyze.

Several sequences contained artifacts that complicated analysis and increased the prevalence of ambiguous base calls. These usually occurred in a predictable pattern and were seen only in a forward or reverse sequence. This may explain the A or C ambiguities, as an A or C call often preceded a large A peak, and was connected to a preceding A shoulder, with a sharp C peak overlapping the shoulder. Another common artifact was a sharp C peak in the middle of a run of three or more A base calls.

One sequencing artifact that is well-characterized is pull-up, which results from spectral overlap of the dyes used in the sequencing reaction (Butler 2005). If the amount of template DNA is too high, it creates an overly high signal for the software to analyze. As a result, one or more small peaks may be observed underneath a high-signal peak on the electropherogram. This was frequently seen in the form of a C pull-up peak underneath a large A peak or as a G peak underneath a large T peak. Pull-up peaks that

were called as two bases by the CEQ software were reviewed and edited to remove the artifact base. If pull-up was extensive in a sequence, the sample was run again using a shorter injection time, which reduced the overall signal, lessening the background and pull-up.

A final sequencing artifact that was occasionally observed was extra peaks that were irregularly shaped or unevenly spaced within a sequence and partially overlapped larger peaks. Most of these were G's and were limited to individual bone sequences and only a forward or reverse sequence. This resulted from a high baseline noise level, causing the analysis software to insert bases. The extra peaks were easily recognizable and were removed in BioEdit once the forward and reverse sequences were aligned.

Conclusions

Difficulties encountered in processing the remains from the Triconch Palace and Merchant's House allowed augmentation of protocols for analysis of DNA from ancient skeletal material. Beyond these purely technical recommendations however, unique information about the Triconch Palace as a burial site was generated. The results detailed here indicate that several of the individuals within the Triconch Palace were buried in family units. The number of shared mtDNA haplotypes in the Palace suggests it was used as a burial plot by at least three maternal lineages. On the other hand, the large number of young children with distinct haplotypes, spatially separated from other individuals, suggests that a second burial system was present, and that diverse people used the Triconch Palace as a cemetery. Individuals with unique haplotypes may have

been buried by outsiders passing along the Vivari Channel, as travel through the waterway was common, and interestingly, these burials were located near the channel side of the Palace. Alternatively, part of the Palace may have acted as a child cemetery, based on the large proportion of unique haplotypes found in very young children. Through the presence of both familial clusters and remains with unique haplotypes, one can infer that the Triconch Palace had dual usage as a burial site. This is a novel finding as it was not a consideration from archaeological and anthropological studies alone. DNA analysis of the ancient remains from the Triconch Palace and Merchant's House has revealed information about familial relatedness, and has sparked an entirely new discussion on the use of the Palace for burial. The application of molecular techniques to the analysis of ancient burials has proven to be a noteworthy tool to complement studies by archaeologists and anthropologists.

APPENDIX A

Table 10: HVII Sequences for Individual Bone Samples

HVII sequences for each bone as compared to the Cambridge Reference Sequence (CRS). Burial numbers are listed in the firs3 column. If multiple bones from a burial were analyzed, the bone type is indicated by an abbreviation following the burial number. A difference from the CRS at a position is indicated by an abbreviation for a nucleotide (for nucleotide see Table 13). Grey boxes indicate regions of sequence that were not obtained.

	73	90	91	95	111	114	116	128	134	137	139	146	150	152	153	155	158	159	167	182	184	185
CRS	A	G	C	A	A	C	A	C	T	A	T	T	C	T	A	T	T	T	C	C	G	G
1185																						
1187 ra																						
1187 fib																						
1188 h	G												T									
1188 p													T									
1224 p													T									
1224 h								S			K		T			K	Y	Y				
1225 p																						
1226 fib																						
1229 h																						
1264 t														Y						Y		K
1262 fib																	Y	Y			R	
1236 fib		K													G							
1236 u																	Y	Y			R	
1267 p				M	M		M				K					K						
5111 p															G							
5111 fe													T									
1452									W			C										
1456 p																						

Table 10 (continued)

	73	90	91	95	111	114	116	128	134	137	139	146	150	152	153	155	158	159	167	182	184	185
5268 p															R		Y	Y	Y			
5268 fe													T	C								
5641			Y																			
3122 fr														Y								
3126 p								S														
1502 u																						A
1502 t																						
1517 p													Y									
1517 u													T									
1518 fib													Y									
1518 h										M												
1518.3															R							
5010 h													T									
5010 fib													Y	Y								
1406 p													H									
1548 p						Y						Y	Y	Y								
1548 t												C		C								
3018 p																						
3018 ri						Y																
3023 fe																	Y	Y				
3060.1																						
3060.2																	Y	Y				

Table 10 (continued): HVII Sequences for Individual Bone Samples

HVII sequences for each bone as compared to the Cambridge Reference Sequence (CRS). Burial numbers are listed in the first column. If multiple bones from a burial were analyzed, the bone type is indicated by an abbreviation following the burial number (ra-radius, fib-fibula, h-humerus, p-petrous portion, t-tibia, u-ulna, fe-femur, fr-frontal fragment, ri-rib, uk-unkown). A difference from the CRS at a position is indicated by an abbreviation for a nucleotide (A-adenine, G-guanine, C-cytosine, T-thymine, Y-both C and T, R-both A and G, W-both T and A, M-both C and A, S-both C and G, K-both G and T, or N-an unknown nucleotide). Grey boxes indicate regions of sequence that were not obtained.

	186	187	188	189	194	195	198	199	200	204	210	213	214	218	219	225	226	227	228	229	234	237
CRS	C	G	A	A	C	T	C	T	A	T	A	T	A	A	A	G	T	A	G	G	A	A
1185							Y															
1187 ra																						
1187 fib																						
1188 h						C																
1188 p																						
1224 p						C							M	M							M	
1224 h																						
1225 p				M				C		C	M			M								
1226 fib								C		C												
1229 h																						
1264 t						Y																
1262 fib		R						Y														
1236 fib						C										A	C					
1236 u																						
1267 p																						
5111 p			M	M		C										A		G				
5111 fe																						
1452	M	R																				

Table 10 (continued)

	186	187	188	189	194	195	198	199	200	204	210	213	214	218	219	225	226	227	228	229	234	237
1456 p		R																				
5268 p	M	R				C										A	C					
5268 fe			W																			
5641																						
3122 fr																						
3126 p																						
1502 u																			A	S	C	M
1502 t			R					Y														
1517 p									G													
1517 u						C								M	M							
1518 fib						Y						W										
1518 h								C		Y												
1518 uk						C										A	C					
5010 h						C																
5010 fib					M																	
1406 p																						
1548 p						C																
1548 t						C																
3018 p																						
3018 ri																						
3023 fe																						
3060 uk																						
3060 uk								Y		Y												

Table 10 (continued): HVII Sequences for Individual Bone Samples

HVII sequences for each bone as compared to the Cambridge Reference Sequence (CRS). Burial numbers are listed in the first column. If multiple bones from a burial were analyzed, the bone type is indicated by an abbreviation following the burial number (ra-radius, fib-fibula, h-humerus, p-petrous portion, t-tibia, u-ulna, fe-femur, fr-frontal fragment, ri-rib, uk-unkown). A difference from the CRS at a position is indicated by an abbreviation for a nucleotide (A-adenine, G-guanine, C-cytosine, T-thymine, Y-both C and T, R-both A and G, W-both T and A, M-both C and A, S-both C and G, K-both G and T, or N-an unknown nucleotide). Grey boxes indicate regions of sequence that were not obtained.

	240	246	250	263	267	279	280
CRS	A	T	T	A	T	T	C
1185							
1187 ra				G			
1187 fib				G			
1188 h				G			
1188 p				G			
1224 p							
1224 h				G			
1225 p							
1226 fib				G			M
1229 h				G			M
1264 t							
1262 fib			Y	G			
1236 fib				G			
1236 u				G			

Table 10 (continued)

	240	246	250	263	267	279	280
1267 p				G			M
5111 p				G			M
5111 fe				G			M
1452				G			
1456 p				G			
5268 p				G			
5268 fe	C						
5641				G			
3122 fr				G	W		
3126 p				G			M
1502 u	M	K					
1502 t				G			
1517 p				G			
1517 u				G			
1518 fib		W		G	W		
1518 h			Y	G			
1518 uk				G			
5010 h				G			M
5010 fib				G			
1406 p				G			M
1548 p				G		Y	
1548 t				G			
3018 p				G	W		
3018 ri				G			
3023 fe				G			
3060 uk				G	W		
3060 uk				G			

Table 11: HVI Sequences for Individual Bone Samples

HVII sequences for each bone as compared to the Cambridge Reference Sequence (CRS). Burial numbers are listed in the first column. If multiple bones from a burial were analyzed, the bone type is indicated by an abbreviation following the burial number (ra-radius, fib-fibula, h-humerus, p-petrous portion, t-tibia, u-ulna, fe-femur, fr-frontal fragment, ri-rib, uk-unkown). A difference from the CRS at a position is indicated by an abbreviation for a nucleotide (A-adenine, G-guanine, C-cytosine, T-thymine, Y-both C and T, R-both A and G, W-both T and A, M-both C and A, S-both C and G, K-both G and T, or N-an unknown nucleotide). Grey boxes indicate regions of sequence that were not obtained.

	16056	16058	16080	16082	16087	16093	16095	16102	16106	16120	16124	16126	16129	16133	16135	16138	16144	16145	16146
CRS	C	A	A	C	A	T	C	T	G	A	T	T	G	C	A	A	T	G	A
1185																			
1187ra																			
1187 fib																			
1188 h				M		Y	Y												
1188 p						Y				M						M			
1224 p																			
1224 h																			
1225 p											Y				W	W			
1226 fib																			
1226 u					M								R						
1229 h													R						
1259																			
1264 t																			
1264 fib													R						
1236 fib																			
1236 u						C													
1267 p						K						C		T				A	
5043 p																			

Table 11 (continued)

	16056	16058	16080	16082	16087	16093	16095	16102	16106	16120	16124	16126	16129	16133	16135	16138	16144	16145	16146
5111 p																			
5111 fe														Y					
5189												C							
5268 p																			
5268 fe													A						
5641			W																
1452											Y	Y							R
1456 p																			
3122 t		W				Y													
3122 fr																			
3126 p					M														
1502 u																			
1502 t																			
1517 p																			
1517 u						C													
1518 h																			
5010 fib																			
1406 fe								K	R		C						K		
1548 p	Y	W					Y												
1548 t																			
3018 p																			
3018 ri																			
3023 p																			
3023 fe																			
3060 uk																			

Table 11 (continued): HVI Sequences for Individual Bone Samples

HVII sequences for each bone as compared to the Cambridge Reference Sequence (CRS). Burial numbers are listed in the first column. If multiple bones from a burial were analyzed, the bone type is indicated by an abbreviation following the burial number (ra-radius, fib-fibula, h-humerus, p-petrous portion, t-tibia, u-ulna, fe-femur, fr-frontal fragment, ri-rib, uk-unkown). A difference from the CRS at a position is indicated by an abbreviation for a nucleotide (A-adenine, G-guanine, C-cytosine, T-thymine, Y-both C and T, R-both A and G, W-both T and A, M-both C and A, S-both C and G, K-both G and T, or N-an unknown nucleotide). Grey boxes indicate regions of sequence that were not obtained.

	16148	16149	16150	16157	16161	16163	16164	16165	16171	16174	16175	16178	16179	16180	16186	16187	16189	16198	16199	16223
CRS	C	A	C	T	T	A	A	A	A	C	A	T	C	A	C	C	T	T	T	C
1185																			W	
1187 ra																				
1187 fib							M		N											
1188 h																			W	
1188 p				Y				M												
1224 p																			W	
1224 h																				
1225 p	M	M	M																	
1226 fib																				
1226 u																				
1229 h																				
1259																			W	
1264 t																	C			
1264 fib																				
1236 fib																			W	
1236 u																			W	

Table 11 (continued)

	16148	16149	16150	16157	16161	16163	16164	16165	16171	16174	16175	16178	16179	16180	16186	16187	16189	16198	16199	16223
1267 p																			W	
5043 p																		W		
5111 p																			A	
5111 fe	Y																			
5189						G									T		C		A	
5268 p														M						
5268 fe																				
5641																				
1452																				
1456 p																			W	
3122 t										M	M									
3122 fr										T							Y			
3126 p							W						S							
1502 u												K								
1502 t																	Y			
1517 p																				
1517 u																			W	
1518 h																				
5010 fib																M			W	
1406 fe																	K			
1548 p																				
1548 t					K															
3018 p																				
3018 ri																	Y		W	
3023 p																				
3023 fe																	Y		W	
3060.2																				

Table 12: HVII Consensus Sequences

HVII consensus sequences for each burial as compared to the Cambridge Reference Sequence (CRS). Burial numbers are listed in the first column. A difference from the CRS at a position is indicated by an abbreviation for a nucleotide (A-adenine, G-guanine, C-cytosine, T-thymine, Y-both C and T, R-both A and G, W-both T and A, M-both C and A, S-both C and G, K-both G and T, or N-an unknown nucleotide). Grey boxes indicate regions of sequence that were not obtained.

	73	90	91	95	111	116	128	134	139	146	150	152	153	155	158	159	185	186	187	189	195	198	199	200	204	210	218	225	226	227	228	234	240	250	263	267	279	280
CRS	A	G	C	A	A	A	C	T	T	T	C	T	A	T	T	T	G	C	G	A	T	C	T	A	T	A	A	G	T	A	G	A	A	T	A	T	T	C
1185																						Y																
1187																																			G			
1188	G										T										Y														G			
1224											Y										Y														G			
1225																				M			C		C	M	M											
1226																							C		C									C	G			M
1229																																			G			M
1264																																			G			
1236		K											R								Y							R	Y						G			
1267				M	M	M			K					K																					G			M
5111											Y		R								Y							R		R					G			
1452								W		C								M	R															G			
1456																			R															G			
5268											T	C									Y							R	Y				M		G			
5641			Y																																G			
3122												Y																							G	W		
3126							S																												G			M
1502																	R														R	M			G			
1517											Y										Y			R											G			

Table 12 (continued)

	73	90	91	95	111	116	128	134	139	146	150	152	153	155	158	159	185	186	187	189	195	198	199	200	204	210	218	225	226	227	228	234	240	250	263	267	279	280
1518																					Y		Y					R	Y						G			
5010											Y										Y														G			M
1406											H																								G			M
1548										C		C									C														G		Y	
3018																																			G			
3023															Y	Y																			G			
3060																																			G			

Table 13: HVI Consensus Sequences

HVI consensus sequences for each burial as compared to the Cambridge Reference Sequence (CRS). Burial numbers are listed in the first column. A difference from the CRS at a position is indicated by an abbreviation for a nucleotide (A-adenine, G-guanine, C-cytosine, T-thymine, Y-both C and T, R-both A and G, W-both T and A, M-both C and A, S-both C and G, K-both G and T, or N-an unknown nucleotide). Grey boxes indicate regions of sequence that were not obtained.

	16056	16058	16080	16087	16093	16102	16106	16124	16126	16129	16133	16135	16138	16144	16145	16146	16148	16149	16150	16163	16164	16165	16174	16179	16186	16187	16189	16198	16199
CRS	C	A	A	A	T	T	G	T	T	G	C	A	A	T	G	A	C	A	C	A	A	A	C	C	C	C	T	T	T
1185																													W
1187																													
1188					C																								W
1224																													
1225								C				W	W				M	M	M										
1226																													
1229										A																			
1259																													W
1264																											Y		
1236					Y																								W
1267					K				C		T				A														W
5043																												W	
5111																													W
5189									C											G					T		C		A
5268										R																			
5641			W																										
1452								Y	Y							R													
1456																													A
3122		W																					H				C		

Table 13 (continued)

	16056	16058	16080	16087	16093	16102	16106	16124	16126	16129	16133	16135	16138	16144	16145	16146	16148	16149	16150	16163	16164	16165	16174	16179	16186	16187	16189	16198	16199
3126				M																	W			S					
1502																													
1517					Y																								
1518																													
5010																										M			W
1406						K	R	C						K													K		
1548	Y	W																											
3018																											Y		W
3023																											Y		W

BIBLIOGRAPHY

Anderson, S., A.T. Bankier, B.G. Barrell, M.H.L. deBruijn, A.R. Coulson, J. Drouin, I.C. Eperon, D.P. Nierlich, B.A. Rose, F. Sanger, R.H. Schreier, A.J.H. Smith, R Staden, and I.G. Young. 1981. Sequence and organization of the human mitochondrial genome. Nature. 290:457 – 465.

Bendall, K.E., V.A. Macaulay, B.C. Sykes. 1997. Variable levels of a heteroplasmic point mutation in individual hair roots. American Journal of Human Genetics. 61:1303 – 1308.

Budowle, B., M.W. Allard and M.R. Wilson. 2002. Critique of interpretation of high levels of heteroplasmy in human mitochondrial DNA hypervariable region I from hair. Forensic Science International. 126:30 – 33.

Butler, J.M. 2005. Forensic DNA Typing: biology, technology, and genetics of STR markers. London: Academic Press.

Butrint, Albania. http://www.history.com/classroom/unesco/butrint/threats.html Accessed Aug 2007.

Butrint Foundation. http://www.butrintfound.dial.pipex.com/ Accessed Aug 2007.

Butrint Foundation. Butrint Foundation Annual Report 2003. http://www.butrintfound.dial.pipex.com/publications/ar03_ebook.pdf. Accessed Aug 2007.

Collins, M.J., C..M. Nielsen–Marsh, J. Hiller, C.I. Smith, J.P. Roberts, R.V. Prigodich, T.J. Wess, J. Csapò, A.R. Millard and G. Turner–Walker. 2002. The survival of organic matter in bone: a review. Archaeometry. 44:383 – 394.

Derevenski, J.S. Children and Material Culture. 2000. Routledge.

Edson, S.M., J.P. Ross, M.D. Coble, T.J. Parsons, and S.M. Barritt. Naming the dead – confronting the realities of rapid identification of degraded skeletal remains. 2004. Forensic Sci Rev. 16:63.

Fenton, T. Personal communication. 2006.

Foran, D. R. 2006. Relative degradation of nuclear and mitochondrial DNA: an experimental approach. Journal of Forensic Sciences. 51: 766 – 770.

Foran, D.R. Personal communication. 2007.

Greenberg, B.D, J.E. Newbold, A. Sugino. 1983. Intraspecific nucleotide sequence variability surrounding the origin of replication in human mitochondrial DNA. Gene. 21:33–49.

Gilbert, M.T., A.J. Hansen, E. Willerslev, L. Rudbeck, I. Barnes, N. Lynnerup, and A. Cooper. 2003. Characterization of genetic miscoding lesions caused by postmortem damage. American Journal of Human Genetics. 72(1):48 – 61.

Hall TA. 1999. BioEdit: a user-friendly biological sequence alignment editor and analysis program for Windows 95/98/NT. Nucl. Acids. Symp. Ser. 41:95-98.

Hodges, R., W. Bowden, O. Gilkes, K. Lako. 2000. Late Roman Butrint, Albania: survey and excavations, 1994 – 98. Archeologia Medievale. XXVII:241 – 257.

Hodges, R., W. Bowden, and K. Lako,. 2004. (eds.) *Byzantine Butrint: Excavations andSurvey 1994-1999.* Oxford, Oxbow.

Hofreiter, M., V. Jaenicke, D. Serre, Av. A. Haeseler, and S. Paabo. 2001. DNA sequences from multiple amplifications reveal artifacts induced by cytosine deamination in ancient DNA. Nucleic Acids Research. 23:4793 – 4799.

Horai, H. and K. Hayasaka. 1990. Intraspecific nucleotide sequence differences in the major noncoding region of human mitochondrial DNA. American Journal of Human Genetics. 46:828 – 842.

Lindahl, T. 1993. Instability and decay of the primary structure of DNA. Nature. 362:709 – 715.

Misner, L. 2004. Predicting mtDNA Quality based on Bone Weathering and Type. Thesis for Degree of M.S. School of Criminal Justice. Michigan State University.

Mutolo, M. 2006. Molecular Identification of Pathogens in Ancient Skeletal Remains From Butrint and Diaporit Albania

Murray, L. 2006. Genetic analysis of the Great Circle from the tumulus at Kamenica, Albania. Thesis for the Degree of M.S. School of Criminal Justice. Michigan State University.

O'Rourke, D.H., G. Hayes, and S.W. Carlyle. 2000. Ancient DNA Studies in Physical Anthropology. Annual Review of Anthropology. 29:217 – 242.

Rennick, S. 2005. Genetic Analysis of Monumental Structure within the Kamenica, Albania Tumulus. Thesis for the Degree of M.S. School of Criminal Justice. Michigan State University.

Rose, H.J. 1922. Celestial and Terrestrial Orientation of the Dead. The Journal of the Royal Anthropological Institute of Great Britain and Ireland. *52*:127 – 140.

Soren, D. Fenton, T. and Birkby, W. The late Roman infant cemetery near Lugnano in Teverina, Italy: some implications, J. Paleopathol., 1995, 7: 13–42.

Theves, C., C. Keyser-Tracqui, E. Crubezy, J.P. Salles, B. Ludes, N. Telmon. 2006. Detection and quantification of the age-related point mutation A189G in the human mitochondrial DNA. Journal of Forensic Sciences. 51:865 – 873.

Tsai, Y. and B.H. Olson. 1992. Detection of low numbers of bacterial cells in soils and sediments by polymerase chain reaction. Applied and Environmental Microbiology. 58:754 – 757.

UNESCO. World Heritage Centre. 2006. http://whc.unesco.org Accessed Aug 2007.

Wilson I. 1997. Inhibition and Facilitation of Nucleic Acid Amplification. Applied and Environmental Microbiology. 63: 3741 – 3751.

Zickel, R. and W.R. Iwaskiw. 1994. Albania: A country study, 2nd Ed. Library of Congress: Federal Research Division.